

PRECEDENCE-CONSTRAINED WINTER VALUE FOR EFFECTIVE GRAPH DATA VALUATION

Hongliang Chi¹, Wei Jin², Charu Aggarwal³, Yao Ma¹

¹Rensselaer Polytechnic Institute, Troy, NY, United States

²Emory University, Atlanta, GA, United States

³IBM T. J. Watson Research Center, Yorktown Heights, NY, United States

{chih3@rpi.edu, wei.jin@emory.edu, charu@us.ibm.com, may13@rpi.edu}

ABSTRACT

Data valuation is essential for quantifying data's worth, aiding in assessing data quality and determining fair compensation. While existing data valuation methods have proven effective in evaluating the value of Euclidean data, they face limitations when applied to the increasingly popular graph-structured data. Particularly, graph data valuation introduces unique challenges, primarily stemming from the intricate dependencies among nodes and the growth in value estimation costs. To address the challenging problem of graph data valuation, we put forth an innovative solution, **Precedence-Constrained Winter (PC-Winter) Value**, to account for the complex graph structure. Furthermore, we develop a variety of strategies to address the computational challenges and enable efficient approximation of PC-Winter. Extensive experiments demonstrate the effectiveness of PC-Winter across diverse datasets and tasks.

1 INTRODUCTION

The abundance of training data has been a key driver of recent advancements in machine learning (ML) (Zhou et al., 2017). As models and the requisite training data continue to expand in scale, data valuation has gained significant attention due to its ability to quantify the usefulness of data for ML tasks and determine fair compensation (Pei, 2020; Sim et al., 2022). Notable techniques in this field include Data Shapley (Ghorbani & Zou, 2019) and its successors (Kwon & Zou, 2021; Wang & Jia, 2023; Schoch et al., 2022), which have gained prominence in assessing data value. Despite the promise of these methods, they are primarily designed for Euclidean data, where samples are often assumed to be independent and identically distributed (i.i.d.). Given the prevalence of graph-structured data in the real world (Fan et al., 2019; Shahsavari & Abbeel, 2015; Li et al.), there arises a compelling need to perform data valuation for graphs. However, due to the interconnected nature of samples (nodes) on graphs, existing data valuation frameworks are not directly applicable to addressing the graph data valuation problem.

In particular, designing data valuation methods for graph-structured data faces several fundamental challenges: **Challenge I:** Graph machine learning algorithms such as Graph Neural Networks (GNNs) (Kipf & Welling, 2016; Veličković et al., 2017; Wu et al., 2019) often involve both labeled and unlabeled nodes in their model training process. Therefore, unlabeled nodes, despite their absence of explicit labels, also hold intrinsic value. Existing data valuation methods, which typically assess a data point's value based on its features and the associated label, do not readily accommodate the valuation of unlabeled nodes within graphs. **Challenge II:** Nodes in a graph contribute to model performance in an interdependent and complex way: (1) Unlabeled nodes, while not providing direct supervision, can contribute to model performance by potentially affecting multiple labeled nodes through message-passing. (2) Labeled nodes, on the other hand, contribute by providing direct supervision signals for model training, and similarly to unlabeled nodes, they also contribute by affecting other labeled nodes through message-passing. **Challenge III:** Traditional data valuation methods are often computationally expensive due to repeated retraining of models (Ghorbani & Zou, 2019). The challenge is magnified in the context of graph-structured data, where samples contribute to

model performance in multifaceted manners. Additionally, the inherent message-passing mechanism in GNN models further amplifies the computational demands for model re-training.

In this work, we make *the first attempt* to explore the challenging graph data valuation problem, to the best of our knowledge. In light of the aforementioned challenges, we propose the **Precedence-Constrained Winter** (PC-Winter) Value, a pioneering approach designed to intricately unravel and analyze the contributions of nodes within graph structures, thereby offering a detailed perspective on the valuation of graph elements. Our key contributions are as follows:

- We formulate the graph data valuation problem as a unique cooperative game (Von Neumann & Morgenstern, 2007) with special coalition structures. Specifically, we decompose each node in the graph into several “players” within the game, each representing a distinct contribution to model performance. We then devise the PC-Winter to address the game, enabling the accurate valuation of all players. The PC-Winter values of these players can be conveniently combined to generate values for nodes and edges.
- To tackle the computational challenges of calculating PC-Winter values, we develop a set of strategies including *hierarchical truncation* and *local propagation*. These strategies together enable an efficient approximation of PC-Winter values.
- Extensive experiments on various datasets and tasks, along with detailed ablation studies and parameter analyses, validate the effectiveness of PC-Winter and provide insights into its behavior.

2 PRELIMINARY AND RELATED WORK

In this section, we delve into some fundamental concepts that are essential for developing our methodology. More extensive literature exploration can be found in Appendix A. For ease of reference, a comprehensive table of notations used throughout this paper is provided in Appendix N.

2.1 COOPERATIVE GAME THEORY

Cooperative game theory explores the dynamics where players, or decision-makers, can form alliances, known as coalitions, to achieve collectively beneficial outcomes (Branzei et al., 2008; Curiel, 2013). The critical components of such a game include a *player set* \mathcal{P} consisting of all players in the game and a *utility function* $U(\cdot)$, which quantifies the value or payoff that each coalition of players can attain. Shapley Value (Shapley et al., 1953) is developed to fairly and efficiently distribute payoffs (values) among players.

Shapley value. The Shapley value $\phi_i(\mathcal{P}, U)$ for a player $i \in \mathcal{P}$ can be defined on permutations of \mathcal{P} as follows.

$$\phi_i(\mathcal{P}, U) = \frac{1}{|\Pi(\mathcal{P})|} \sum_{\pi \in \Pi(\mathcal{P})} [U(\mathcal{P}_i^\pi \cup \{i\}) - U(\mathcal{P}_i^\pi)] \quad (1)$$

where $\Pi(\mathcal{P})$ denotes the set of all possible permutations of \mathcal{P} with $|\Pi(\mathcal{P})|$ denoting its cardinality, and \mathcal{P}_i^π is predecessor set of i , i.e, the set of players that appear before player i in a permutation π :

$$\mathcal{P}_i^\pi = \{j \in \mathcal{P} \mid \pi(j) < \pi(i)\}. \quad (2)$$

The Shapley value considers each player’s contribution to every possible coalition they could be a part of. Specifically, in (1), for each permutation π , the *marginal contribution* of player i is calculated as the difference in the utility function U when player i is added to an existing coalition \mathcal{P}_i^π . The Shapley value $\phi_i(\mathcal{P}, U)$ for i is the average of these marginal contributions across all permutations in $\Pi(\mathcal{P})$. The Shapley value has been widely applied in ML for various tasks such as data valuation (Ghorbani & Zou, 2019; Jia et al., 2019) and model explanation (Liu et al., 2022b; Frye et al., 2020). In the context of graph ML, it has been primarily used for GNN explainability (Duval & Malliaros, 2021; Yuan et al., 2021; Mastropietro et al., 2022; Akkas & Azad, 2024). A more detailed discussion on Shapley Value on graph ML can be found in Appendix A.3.

Winter Value. The Shapley value is to address cooperative games, where players collaborate freely and contribute on an equal footing. However, in many practical cases, cooperative games, exhibit a *Level Coalition Structure* (Niyato et al., 2011; Vasconcelos et al., 2020; Yuan et al., 2016), reflecting a hierarchical organization. For instance, consider a corporate setting where different tiers of management and staff contribute to a project in varying capacities and with differing degrees of

decision-making authority. Players within such a game are hierarchically categorized into nested coalitions with several levels, as depicted in Figure 1. The outermost and largest ellipse represents the entire coalition and each of the smaller ellipse within the largest ellipse symbolizes a “sub-coalition” at various hierarchical levels. Collaborations originate within the smallest sub-coalitions at the base level (illustrated by the innermost ellipses in Figure 1).

These base units are then integrated into the next level, facilitating inter-coalition collaboration and enabling contributions to ascend to higher levels. This bottom-up flow of contributions continues, with each layer consolidating and passing on inputs to the next, culminating in a multi-leveled collaborative contribution to the final objective of the entire coalition. To accommodate such complex Level Coalition Structure, Winter value (Winter, 1989) was introduced. Winter value follows a similar permutation-based definition as Shapley Value ((1)) but with only a specific subset of permutations that respect the Level Coalition Structure. In these permutations, members of the same sub-coalition, regardless of the level, must appear in an unbroken sequence without interruptions. This ensures that the value attributed to each player is consistent with the level structure of the coalition. A formal definition of the Winter value can be found in Appendix B.

2.2 DATA VALUATION AND DATA SHAPLEY

Data valuation quantifies the contribution of data points for machine learning tasks. The seminal work (Ghorbani & Zou, 2019) introduces Data Shapley, applying cooperative game theory to data valuation, where training samples are the *players* \mathcal{P} , and the *utility function* U assesses a model’s performance on subsets of these players using a validation set. With \mathcal{P} and U , data values can be calculated with (1). However, Data Shapley and subsequent methods (Ghorbani & Zou, 2019; Kwon & Zou, 2021; Wang & Jia, 2023) primarily focus on i.i.d. data, overlooking potential coalitions or dependencies among data points.

2.3 GRAPHS AND GRAPH NEURAL NETWORKS

Consider a graph $\mathcal{G} = \{\mathcal{V}, \mathcal{E}\}$ where \mathcal{V} denotes the set of nodes and \mathcal{E} denotes the set of edges. Each node $v_i \in \mathcal{V}$ carries a feature vector $\mathbf{x}_i \in \mathbb{R}^d$, where d is the dimensionality of the feature space. Additionally, each node v_i is associated with a label y_i from a set of possible labels \mathcal{C} . We assume that only a subset $\mathcal{V}_l \subset \mathcal{V}$ are with known labels.

GNNs (Kipf & Welling, 2016; Veličković et al., 2017; Wu et al., 2019) are prominent models for graph ML tasks. Specifically, from a local perspective for node v_i , the k -th GNN layer generally performs a feature averaging process as $\mathbf{h}_i^{(k)} = \frac{1}{\deg(v_i)} \sum_{v_j \in \mathcal{N}(v_i)} \mathbf{W} \mathbf{h}_j^{(k-1)}$, where \mathbf{W} is the parameter

matrix, $\deg(v_i)$ and $\mathcal{N}(v_i)$ denote the degree and neighbors of node v_i , respectively. After a total of K layers, $\mathbf{h}_i^{(K)}$ are utilized as the learned representation of v_i . Such a feature aggregation process can be also described with a K -level *computation tree* (Jegelka, 2022) rooted on node v_i .

Definition 1 (Computation Tree). *For a node $v_i \in \mathcal{V}$, its K -level computation tree corresponding to a K -layer GNN model is denoted as \mathcal{T}_i^K with v_i as its root node. The first level of the tree consists of the immediate neighbors of v_i , and each subsequent level is formed by the neighbors of nodes in the level directly above. This pattern of branching out continues, expanding through successive levels of neighboring nodes until the depth of the tree grows to K .*

The feature aggregation process in a K -layer GNN can be regarded as a bottom-up feature propagation process in the computation tree, where nodes in the lowest level are associated with their initial features. Therefore, the final representation $\mathbf{h}_i^{(K)}$ of a node v_i is affected by all nodes within its K -hop neighborhood, which is referred to as the *receptive field* of node v_i . The GNN model is trained using the $(\mathbf{h}_i^{(K)}, y_i)$ pairs, where each labeled node v_i in \mathcal{V}_l is represented by its final representation and corresponding label. *Thus, in addition to labeled nodes, those unlabeled nodes that are within the receptive field of labeled nodes also contribute to model performance.*

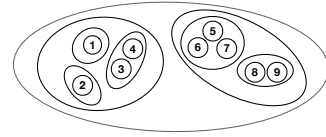


Figure 1: Level Coalition Structure

3 METHODOLOGY

Machine learning models designed for Euclidean data traditionally assume independent and identically distributed (i.i.d.) samples, where the contribution of each labeled sample to model performance manifests through direct supervision signals. In contrast, graph-structured data presents fundamentally different contribution patterns due to the interdependencies between nodes. Specifically, as discussed in Section 2.3, both labeled and unlabeled nodes are involved in the training stage through the feature aggregation. Next, we discuss how these nodes contribute to GNN performance.

Observation 1. *Unlabeled nodes influence GNN performance by affecting the final representation of labeled nodes. On the other hand, labeled nodes can contribute to GNN performance in two ways: (1) they provide direct supervision signals to GNN with their labels, and (2) just like unlabeled nodes, they can impact the final representation of other labeled nodes through feature aggregation. Note that both labeled nodes and unlabeled nodes can affect the final representations of multiple labeled nodes, as long as they lie within the receptive field of these labeled nodes. Hence, a single node can make multifaceted and heterogeneous contributions to GNN performance by affecting multiple labeled nodes in various manners.*

3.1 THE GRAPH DATA VALUATION PROBLEM

Based on Observation 1, due to the heterogeneous and diverse effects of labeled and unlabeled nodes, it is necessary to perform fine-grained data valuation on graph data elements. In particular, we propose to decompose a node into distinct ‘‘duplicates’’ corresponding to their impact on different labeled nodes. The fundamental objective is to quantify the value of these duplicates in a way that captures their unique roles in the message-passing process. Following existing literature (Ghorbani & Zou, 2019; Wang & Jia, 2023; Yan & Procaccia, 2021), we approach the graph data value problem through a cooperative game.

Definition 2 (Player Set). *The player set \mathcal{P} in a graph data valuation game is defined as the union of nodes in the computation trees of labeled nodes. Duplication of nodes may occur within a single computation tree \mathcal{T}_i^K or across different labeled nodes’ computation trees. In the graph data valuation game, these potential duplicates are treated as distinct players, uniquely identified by their paths to the corresponding labeled node. We define the player set \mathcal{P} as the set of all these distinct players across the computation trees of all labeled nodes in \mathcal{V}_l .*

Definition 3 (Utility Function). *Given a subset $\mathcal{S} \subset \mathcal{P}$, we first generate a node-induced graph $G_{in}(\mathcal{S})$ using their corresponding edges in the computation trees. Then, a GNN model \mathcal{A} is trained on the induced graph $G_{in}(\mathcal{S})$. Its performance is evaluated on a held-out validation set to serve as the utility of \mathcal{S} , calculated as $U(\mathcal{S}) = acc(\mathcal{A}(G_{in}(\mathcal{S})))$, where acc measures the accuracy of the trained GNN model $\mathcal{A}(G_{in}(\mathcal{S}))$ on a held-out validation set.*

The goal of the graph data valuation problem is to assign a value to all players in \mathcal{P} with the help of the *utility function* U . When calculated properly, these values are supposed to provide a detailed understanding of how players in \mathcal{P} contribute to the GNN performance in a fine-grained manner. Furthermore, these values can be flexibly combined to generate higher-level values for nodes and edges, which will be discussed in Section 3.5.

3.2 PRECEDENCE-CONSTRAINED WINTER VALUE

As discussed in Section 2.3, the final representations of a labeled node v_i come from the hierarchical collaboration of all players in the computation tree \mathcal{T}_i^K . These labeled nodes with the updated representations then contribute to the GNN performance through the training objective. Such a contribution process forms a hierarchical collaboration between the players in \mathcal{P} , which can be illustrated with a *contribution tree* \mathcal{T} as shown in Figure 2a. In particular, the *contribution tree* \mathcal{T} is constructed by linking the root nodes of the computation trees of all labeled nodes with a dummy node representing the GNN training objective \mathcal{O} . In Figure 2a, for the ease of illustration, we set $K = 2$, include only 2 labeled nodes, i.e., v_0, v_1 , and utilize w_i, u_i to denote the nodes in the lower level. The subtree rooted at a labeled node $v_i \in \mathcal{V}$ is the corresponding computation tree \mathcal{T}_i^2 . With this, we observe the following about the coalition structure of the graph data valuation game.

Observation 2 (Level Coalition Structure). *As shown in Figure 2a, the players in \mathcal{P} hierarchically collaborate to contribute. At the bottom level, the players are naturally grouped by their parents.*

Specifically, players with a common parent such as u_0, u_1, u_2 with their parent w_0 , establish a foundation sub-coalition. This sub-coalition is clearly depicted in Figure 2b. Moving up the tree, these parent nodes, like w_0 , serve as “delegates” for their respective sub-coalitions, further engaging in collaborations with other sub-coalitions. This interaction forms higher-level sub-coalitions, such as the one between w_0, w_1, w_2 , and v_0 in Figure 2b, indicating inter-coalition cooperation. This ascending process of coalition formation continues until the root node \mathcal{O} is reached, which represents the objective of the entire coalition consisting of all players. The depicted hierarchical collaboration process aligns with the Level Coalition Structure discussed in Section 2.1.

While the contribution tree shares similarities with the Level Coalition Structure illustrated in Section 2.1, a pivotal distinction lies in the representation and function of “delegates” (highlighted in red in Figure 2b) within each coalition. In the traditional Level Coalition Structure, contributions within a sub-coalition are made collectively, with each player or lower-level sub-coalition participating on an equitable basis. In contrast, the contribution tree framework distinguishes itself by designating a “delegate” within each sub-coalition, a player that represents and advances the collective contributions, establishing a directed and tiered flow of influence, hence forming a Unilateral Dependency Structure.

Observation 3 (Unilateral Dependency Structure). *In the contribution tree framework, a player $p \in \mathcal{P}$ contributes to the final objective through a hierarchical pathway facilitated by its ancestors (its “delegates” at different levels). Therefore, the collaboration between players in \mathcal{P} exhibits a Unilateral Dependency Structure, where a player p ’s contribution is dependent on its ancestors.*

According to these two observations, the players demonstrate unique coalition structures in the graph data valuation game. We aim to propose a permutation-based valuation framework similar to (1) to address the cooperative game with both Level Coalition Structure and Unilateral Dependency Structure. In particular, instead of utilizing all the permutations as in (1), only the *permissible permutations* aligning with such coalition structures are included in the value calculations. As we described in Section 2.1, cooperative games with Level Coalition Structure have been addressed by the Winter value (Winter, 1989; Chantreuil, 2001). Specifically, a permutation respecting the Level Coalition Structure must ensure that players in the same (sub-)coalition, regardless of its level, are grouped together without interruption from other players (Winter, 1989). In our scenario, any subtree of the contribution tree corresponds to a sub-coalition as demonstrated in Figure 2. Hence, we need to ensure that for any player $p \in \mathcal{P}$, the player p and its descendants in the contribution tree should be grouped together in the permutation. For example, the players w_0, u_0, u_1, u_2 should present together as a group in the permutation with potentially different orders. On the other hand, to ensure the Unilateral Dependency Structure, a permutation must maintain a partial order. Specifically, for any player p in the permutation, its descendants must present in later positions in the permutation than p . Otherwise, the descendants of p cannot make non-trivial contributions, resulting in 0 marginal contributions.

We formally define the *permissible permutations* that align with both Level Coalition Structure and Unilateral Dependency Structure utilizing the following two constraints.

Constraint 1 (Level Constraint). *For any player $p \in \mathcal{P}$, the set of its descendants in the contribution tree is denoted as $\mathcal{D}(p)$. Then, a permutation π aligning with the Level Coalition Structure satisfies the following Level Constraint: $|\pi[i] - \pi[j]| \leq |\mathcal{D}(p)|, \forall i, j \in \mathcal{D}(p) \cup p, \forall p \in \mathcal{P}$, where $\pi[i]$ denotes the positional rank of the i in π .*

Constraint 2 (Precedence Constraint). *A permutation π aligning with the Unilateral Dependency Structure satisfies the following Precedence Constraint: $\pi[p] < \pi[i], \forall i \in \mathcal{D}(p), \forall p \in \mathcal{P}$.*

We denote the set of *permissible permutations* satisfying both *Level Constraint* and *Precedence Constraint* as Ω . Then, we define the **Precedence-Constrained Winter** (PC-Winter) value for a

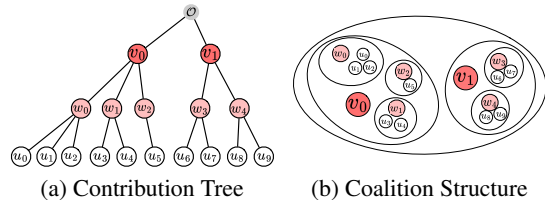


Figure 2: Graph Data Valuation Game Structure

player $p \in \mathcal{P}$ with the permutations in Ω as follows.

$$\psi_p(\mathcal{P}, U) = \frac{1}{|\Omega|} \sum_{\pi \in \Omega} (U(\mathcal{P}_p^\pi \cup p) - U(\mathcal{P}_p^\pi)), \quad (3)$$

where $U(\cdot)$ is the utility function (see Definition 3), and \mathcal{P}_p^π denotes the predecessor set of p in π as defined in (2).

3.3 PERMISSIBLE PERMUTATIONS FOR PC-WINTER

To calculate PC-Winter value, it is required to obtain all permissible permutations. A straightforward way is to enumerate all permutations and only retain the permissible permutations. However, such an approach is extremely computationally intensive and typically not feasible in reality. In this section, to address this challenge, we propose a novel method to directly generate these permutations by traversing the contribution tree with Depth-First Search (DFS). Specifically, each DFS traversal results in a *preordering*, which is a list of the nodes (players) in the order that they were visited by DFS. Such a *preordering* naturally defines a permutation of \mathcal{P} by simply removing the dummy node in the contribution tree from the *preordering*. By iterating all possible DFS traversals of the contribution tree, we can obtain all permutations in Ω , which is demonstrated in the following theorems.

Theorem 1 (Specificity). *Given a contribution tree \mathcal{T} with a set of players \mathcal{P} , any DFS traversal over the \mathcal{T} results in a permissible permutation of \mathcal{P} that satisfies both the Level Constraint and Precedence Constraint.*

Theorem 2 (Exhaustiveness). *Given a contribution tree \mathcal{T} with a set of players \mathcal{P} , any permissible permutation $\pi \in \Omega$ can be generated by a corresponding DFS traversal of \mathcal{T} .*

The proofs for two theorems can be found in Appendix C. Theorem 1 demonstrates that DFS traversals *specifically* generate *permissible permutations*. On the other hand, Theorem 2 ensures the *exhaustiveness* of generation, which allows us to obtain all permutations in Ω by DFS traversal. Together, these two theorems ensure us to *exactly* generate the set of *permissible permutations* Ω .

Notably, the calculation of PC-Winter value involves two steps: 1) generating Ω with DFS traversals; and 2) calculating the PC-Winter value according to (3). Nonetheless, it can be done in a streaming way while we perform the DFS traversals. Specifically, once we reach a player p in a DFS traversal, we can immediately calculate its marginal contribution. The PC-Winter values for all players are computed by averaging their marginal contributions from all possible DFS traversals.

3.4 EFFICIENT APPROXIMATION OF PC-WINTER

Calculating the PC-Winter value for players in \mathcal{P} is infeasible due to computational intensity, arising from: 1) The exponential growth in the number of permissible permutations with more players, rendering exhaustive enumeration intractable; 2) The necessity to re-train the GNN within the utility function for each permutation, a process repeated $|\mathcal{P}|$ times to account for every player’s marginal contribution; and 3) The intensive computation involved in GNN re-training, requiring feature aggregation over the graph that increases in complexity with the graph’s size. These challenges necessitate an efficient approximation method for PC-Winter valuation in practical applications. We propose three strategies to address these computational issues.

3.4.1 PERMUTATION SAMPLING

Following Data Shapley (Ghorbani & Zou, 2019), we adopt Monte Carlo (MC) sampling to randomly sample a subset of *permissible permutations* denoted as Ω_s . This sampling approach maintains the structural properties of permutations while significantly reducing computational overhead. Then, we utilize Ω_s to replace Ω in (3) for approximating PC-Winter value.

3.4.2 HIERARCHICAL TRUNCATION

While permutation sampling reduces the number of evaluations, the computational cost for each evaluation remains substantial. GNN models often demonstrate a phenomenon of *neighborhood saturation*, i.e, these models achieve satisfactory performance even when trained on a subgraph using only a small subset of neighbors, rather than the full neighborhood (Hamilton et al., 2017;

Liu et al., 2021; Ying et al., 2018; Chen et al., 2017), indicating diminishing returns from additional neighbors beyond a certain point. This indicates that for a player p in a permissible permutation π generated by DFS over the contribution tree, the marginal contributions of its late visited child players are insignificant. Thus, we propose hierarchical truncation for efficiently obtaining the marginal contributions by directly approximating insignificant values as 0.

Specifically, during the DFS traversal, given a truncation ratio r , we only compute actual marginal contributions for players in the first $1 - r$ portion of each node’s child subtrees, approximating the marginal contributions of players in the remaining subtrees as 0. For example, in Figure 2a, given a truncation ratio $r = 2/3$, when DFS reaches player v_0 , we only calculate marginal contributions for players in the subtree rooted at w_0 . Furthermore, in the subtree rooted at w_0 , due to the hierarchical truncation, only the marginal contribution of u_0 is evaluated, those for node u_1 and u_2 are set to 0.

This approach is further optimized by adjusting truncation ratios based on the tree level, accommodating varying contribution patterns across levels. In particular, we organize the pair of truncation ratio as r_1-r_2 , indicating we truncate r_1 (or r_2) portion of subtrees (or child players) of v_i (or w_i). We show how the hierarchical truncation helps tremendously reduce the model re-training in Appendix D.

3.4.3 LOCAL PROPAGATION

To enhance scalability, we leverage SGC (Wu et al., 2019) in our utility function, which simplifies GNNs by aggregating node features before applying an MLP. According to the Level Constraint (Constraint 1), the players within the same computation tree are grouped together in the permutation. Therefore, the induced graph of any coalition \mathcal{P}_p^π defined by a permissible permutation consists of a set of separated computation trees (or a partial computation tree corresponding to the last visited labeled node in \mathcal{P}_p^π).

A key observation is that the feature aggregation process for the labeled nodes can be done independently within their own computation trees. Hence, instead of performing the feature propagation for the entire induced graph, we propose to perform *local propagation* only on necessary computation trees. In particular, the aggregated representation for a labeled node is fixed after we traverse its entire computation tree in DFS. Therefore, for evaluating a player p ’s marginal contribution, only the partial computation tree of the last visited labeled node requires *local propagation*, minimizing feature propagation efforts.

To summarize, the PC–Winter values for all players are efficiently approximated using a combination of three strategies in a streaming manner. In particular, we randomly traverse the contribution tree with DFS for $|\Omega_s|$ times. During each DFS traversal, the marginal contributions for all players in \mathcal{P} are efficiently obtained with the help of *hierarchical truncation* and *local propagation*. The marginal contributions calculated through these $|\Omega_s|$ DFS traversals are averaged to approximate the PC–Winter value for all players. In Appendix I.5, we provide a detailed complexity analysis of the PC–Winter algorithm. More details of the PC–Winter framework, including its visual overview of its approximation procedure, are presented in Appendix M.

3.5 FROM PC–WINTER TO NODE AND EDGE VALUES

The PC–Winter values for players in \mathcal{P} can be flexibly combined to obtain the values for elements in the original graph. This section illustrates how to derive both node-level and edge-level valuations from our player-centric framework.

As discussed in Section 3.1, multiple “duplicates” of a node $v \in \mathcal{V}$ in the original graph may potentially present in \mathcal{P} . To capture a node’s overall contribution, we define the *node value* for node v by summing the PC–Winter values of all its “duplicates” in \mathcal{P} . This aggregation naturally combines the different roles a node plays in contributing to model performance.

From a structural perspective, each player (except for the rooted labeled players) in \mathcal{P} corresponds to an “edge” in the contribution tree, identified by the player and its parent. For instance, in Figure 2a, the player u_0 corresponds to the “edge” connecting u_0 and w_0 . Through this lens, DFS traversals generate permutations not just for players, but implicitly for these “edges” as well. The marginal contribution calculated for a player p through a DFS traversal can thus be interpreted as the marginal contribution of its corresponding edge, viewing the process as gradually adding “edges” to connect the players in \mathcal{P} .

Similar to nodes, an edge $e \in \mathcal{E}$ in the original graph may have multiple “duplicates” in the contribution tree, each representing a different pathway of influence. Therefore, we define the *edge value* for $e \in \mathcal{E}$ by taking the summation of the `PC-Winter` value for all its “duplicates” in the contribution tree. This aggregation captures the total impact of each edge in facilitating information flow across the graph.

4 EXPERIMENT

Datasets and Settings. We assess the proposed approach on six real-world benchmark datasets: Cora, Citeseer, and Pubmed Sen et al. (2008), Amazon-Photo, Amazon-Computer, and Coauthor-Physics Shchur et al. (2018). The detailed statistics of datasets are summarized in Table 2 in Appendix G. Our experiments focus on the inductive node classification task. The detailed setup of the inductive setting can be found in Appendix G.1. To obtain the `PC-Winter` values, we run permutations in a streaming way as described in Section 3.4. This process terminates with a convergence criterion as detailed in Appendix G.4. `PC-Winter` typically terminates with a different number of permutations for different datasets. The other hyper-parameters are detailed in Appendix G.5.

4.1 DROPPING HIGH-VALUE NODES

In this section, we aim to evaluate the quality of data values produced by `PC-Winter` via dropping high-value nodes from the graph. Dropping high-value nodes is expected to significantly diminish performance, and thus the performance observed after removing high-value nodes serves as a strong indicator of the efficacy of graph data valuation. Notably, `PC-Winter` values values are calculated as described in Section 3.5.

To demonstrate the effectiveness of `PC-Winter`, we include Random value, Degree value, Leave-one-out (LOO) value, and Data Shapley value as baselines. A more detailed description of these baselines is included in Appendix G.6. To conduct node-dropping experiments, nodes are ranked by their assessed values for each method and removed sequentially from the training graph \mathcal{G}_{tr} . After each removal, we train a GNN model based on the remaining graph and evaluate its performance on the testing graph \mathcal{G}_{te} . Performance changes are depicted through a curve that tracks the model’s accuracy as nodes are progressively eliminated. Labeled nodes often contribute more significantly to model performance than unlabeled nodes because they directly offer supervision. Thereby, with accurately assigned node values, labeled nodes should be prioritized for removal over unlabeled nodes. We empirically validate this hypothesis in Figure 6, discussed in Appendix E. Specifically, in nearly all datasets, our observations reveal that the majority of labeled nodes are removed prior to the unlabeled nodes by both `PC-Winter` and Data Shapley. This leads to a plateau in the latter portion of the performance curves since a GNN model cannot be effectively trained with only unlabeled nodes. Consequently, this scenario significantly hampers the ability to assess the value of unlabeled nodes. Therefore, we propose to conduct separate assessments for the values of labeled and unlabeled nodes. Here, we only include the results for unlabeled nodes, while the results for labeled nodes are presented in Appendix F.

Results and Analysis. Figure 3 illustrates the performance comparison between `PC-Winter` and other baselines across various datasets. From Figure 3, we make the following observations. First, the removal of high-value unlabeled nodes identified by `PC-Winter` consistently results

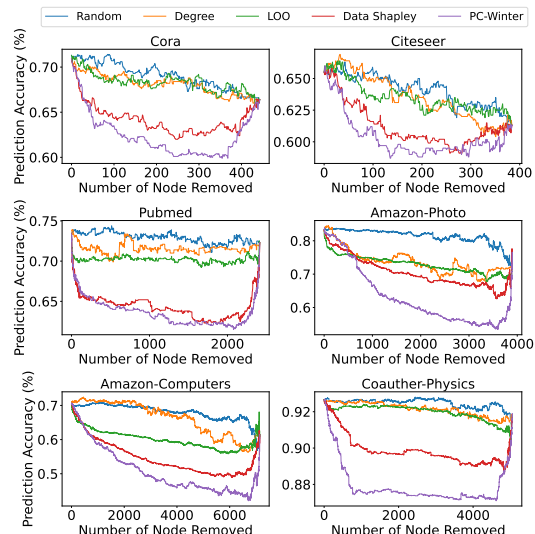


Figure 3: Dropping High-Value Nodes

in the most significant decline in model performance across various datasets. This is particularly evident after removing a relatively small fraction (10%-20%) of the highest-value nodes. This trend underscores the importance of high-value nodes. Notably, in most datasets PC-Winter outperforms the best baseline method, Data Shapley, by a considerable margin, highlighting its effectiveness. Second, the decrease in performance caused by our method is not only substantial but also persistent throughout the node-dropping process, further validating the effectiveness of PC-Winter. Third, the performance curves of PC-Winter and Data Shapley eventually rebound towards the end. This rebound corresponds to the removal of unlabeled nodes that make negative contributions. Their removal aids in improving performance, ultimately reaching the MLP performance when all nodes are excluded. This upswing not only evidences the discernment of PC-Winter and Data Shapley in ascertaining node values but also showcases the particularly acute precision of PC-Winter. These insights collectively affirm the capability of PC-Winter in accurately assessing node values. For a detailed quantitative analysis of these results, including minimum and mean accuracies across all datasets, please refer to Tables 4 and 5 in Appendix H. Furthermore, we extend our evaluation to regression tasks and class-balanced accuracy metrics in Appendices J and K respectively, demonstrating the effectiveness of PC-Winter across different learning scenarios.

4.2 ADDING HIGH-VALUE EDGES

In this section, we explore the impact of adding high-value elements to a graph, providing an alternative perspective to validate the effectiveness of data valuation. Notably, adding high-value nodes to a graph typically involves the concurrent addition of edges, which complicates the addition process. Thus, we target the addition of high-value edges, providing a complementary perspective to our analysis. As described in Section 3.5, the flexibility of PC-Winter allows for obtaining edge values without a separate “reevaluation” process for edges.

Here, we keep all nodes in \mathcal{G}_{tr} and sequentially add edges according to the edge values in descending order, starting with the highest-valued ones. Similar to the node-dropping experiments, the effectiveness of the edge addition is shown through performance curves. We include Random value, Edge-Betweenness, Leave-one-out (LOO) as baselines. Notably, here, Random and LOO specifically pertain to edges, and while we use the same terminology as in the prior section, they are distinct methods, which are detailed in Appendix G.6.

Results and Analysis. Figure 4 illustrates that the Random, LOO, and Edge-Betweenness baselines achieve only linear performance improvements with the addition of more edges, failing to discern the most impactful ones for a sparse yet informative graph. In contrast, the inclusion of edges based on the PC-Winter value results in a steep performance climb, affirming the PC-Winter’s efficacy in pinpointing key edges. Notably, the Cora dataset reaches full-graph performance using merely 8% of the edges selected by PC-Winter. Moreover, with just 10% of PC-Winter-selected edges, the accuracy climbs to 72.9%, outperforming the full graph’s 71.3%, underscoring PC-Winter’s capability to identify valuable edges. This trend is generally consistent across other datasets as well. A comprehensive quantitative analysis of the edge addition results, including maximum and mean accuracies for all methods and datasets, can be found in Tables 6 and 7 in Appendix H.

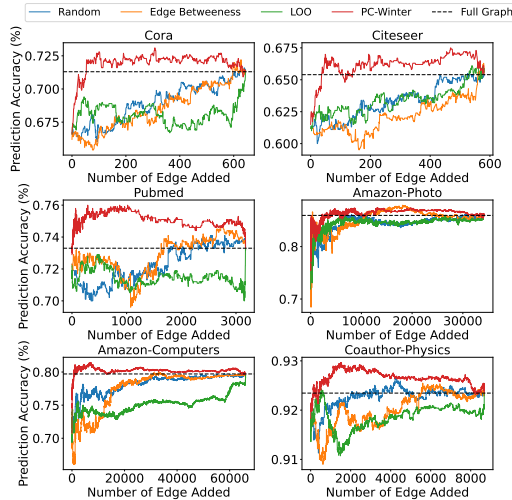


Figure 4: Adding the High-Value Edges

4.3 ABLATION STUDY, PARAMETER AND EFFICIENCY ANALYSIS

In this section, we conduct an ablation study, parameter analysis, and efficiency analysis to gain deeper insights into PC-Winter using node-dropping experiments.

Ablation Study. We conduct an ablation study to understand how the two constraints in Section 3.2 affect the effectiveness of PC-Winter. We introduce two variants of PC-Winter by lifting one of the constraints for the permutations. In particular, we define PC-Winter-L using the permutations satisfying the Level Constraint. Similarly, PC-Winter-P is defined with permutations only satisfying Precedence Constraint. As shown in Figure 5, PC-Winter value outperforms the PC-Winter-L and PC-Winter-P on both datasets, which demonstrates that both constraints are crucial for PC-Winter. Additional results on other datasets are provided in Appendix I.1.

Parameter Analysis. We conduct parameter analyses to investigate the impact of permutation number and truncation ratios on PC-Winter’s performance. The results reveal that PC-Winter achieves robust performance even with a significantly reduced number of permutations and high truncation ratios. Detailed findings are presented in Appendix I.2 and Appendix I.3, respectively.

Efficiency Analysis. We compare the efficiency of PC-Winter and Data Shapley. Analysis of converged permutation count and time per permutation across 6 datasets underscores PC-Winter’s significantly higher efficiency. A comprehensive breakdown is available in Appendix I.4.

5 CONCLUSION

In this paper, we introduce PC-Winter, an innovative approach for effective graph data valuation. The method is specifically designed for graph-structured data and addresses the challenges posed by unlabeled elements and complex node dependencies within graphs. Furthermore, we introduce a set of strategies for reducing the computational cost, enabling efficient approximation of PC-Winter. Extensive experiments demonstrate the practicality and effectiveness of PC-Winter in various datasets and tasks. While PC-Winter demonstrates improved efficiency compared to Data Shapley, we acknowledge that further efficiency enhancements are crucial to fully unlock the potential of graph data valuation in real-world applications. Our work can be seen as a foundation for future research in this direction.

ACKNOWLEDGMENTS

We thank Prof. Lirong Xia from Rutgers University for his valuable discussions and insights that helped improve this work. The research is supported by the National Science Foundation (NSF) under grant numbers NSF2406647 and NSF-2406648.

REFERENCES

- Selahattin Akkas and Ariful Azad. Gnnshap: Scalable and accurate gnn explanation using shapley values. In *Proceedings of the ACM on Web Conference 2024*, pp. 827–838, 2024.
- Piotr Bielak, Tomasz Kajdanowicz, and Nitesh V Chawla. Graph barlow twins: A self-supervised representation learning framework for graphs. *Knowledge-Based Systems*, 256:109631, 2022.
- Rodica Branzei, Dinko Dimitrov, and Stef Tijs. *Models in cooperative game theory*, volume 556. Springer Science & Business Media, 2008.
- Joan Bruna, Wojciech Zaremba, Arthur Szlam, and Yann LeCun. Spectral networks and locally connected networks on graphs. *arXiv preprint arXiv:1312.6203*, 2013.

Hongyun Cai, Vincent W Zheng, and Kevin Chen-Chuan Chang. Active learning for graph embedding. *arXiv preprint arXiv:1705.05085*, 2017.

Frédéric Chantreuil. Axiomatics of level structure values. *Power Indices and Coalition Formation*, pp. 45–62, 2001.

Jianfei Chen, Jun Zhu, and Le Song. Stochastic training of graph convolutional networks with variance reduction. *arXiv preprint arXiv:1710.10568*, 2017.

Zizhang Chen, Peizhao Li, Hongfu Liu, and Pengyu Hong. Characterizing the influence of graph elements. *arXiv preprint arXiv:2210.07441*, 2022.

Hongliang Chi and Yao Ma. Enhancing contrastive learning on graphs with node similarity. In *Proceedings of the 30th ACM SIGKDD Conference on Knowledge Discovery and Data Mining*, pp. 456–465, 2024.

Hongliang Chi, Cong Qi, Suhang Wang, and Yao Ma. Active learning for graphs with noisy structures. In *Proceedings of the 2024 SIAM International Conference on Data Mining (SDM)*, pp. 262–270. SIAM, 2024.

Imma Curiel. *Cooperative game theory and applications: cooperative games arising from combinatorial optimization problems*, volume 16. Springer Science & Business Media, 2013.

Yushun Dong, Ninghao Liu, Brian Jalaian, and Jundong Li. Edits: Modeling and mitigating data bias for graph neural networks. In *Proceedings of the ACM web conference 2022*, pp. 1259–1269, 2022a.

Yushun Dong, Song Wang, Yu Wang, Tyler Derr, and Jundong Li. On structural explanation of bias in graph neural networks. In *Proceedings of the 28th ACM SIGKDD Conference on Knowledge Discovery and Data Mining*, pp. 316–326, 2022b.

Yushun Dong, Song Wang, Jing Ma, Ninghao Liu, and Jundong Li. Interpreting unfairness in graph neural networks via training node attribution. In *Proceedings of the AAAI conference on artificial intelligence*, volume 37, pp. 7441–7449, 2023.

Alexandre Duval and Fragkiskos D Malliaros. Graphsvx: Shapley value explanations for graph neural networks. In *Machine Learning and Knowledge Discovery in Databases. Research Track: European Conference, ECML PKDD 2021, Bilbao, Spain, September 13–17, 2021, Proceedings, Part II 21*, pp. 302–318. Springer, 2021.

Edoardo D’Amico, Khalil Muhammad, Elias Tragos, Barry Smyth, Neil Hurley, and Aonghus Lawlor. Item graph convolution collaborative filtering for inductive recommendations. In *European Conference on Information Retrieval*, pp. 249–263. Springer, 2023.

Wenqi Fan, Yao Ma, Dawei Yin, Jianping Wang, Jiliang Tang, and Qing Li. Deep social collaborative filtering. In *Proceedings of the 13th ACM RecSys*, 2019.

Christopher Frye, Damien de Mijolla, Tom Begley, Laurence Cowton, Megan Stanley, and Ilya Feige. Shapley explainability on the data manifold. *arXiv preprint arXiv:2006.01272*, 2020.

Johannes Gasteiger, Aleksandar Bojchevski, and Stephan Günnemann. Predict then propagate: Graph neural networks meet personalized pagerank. *arXiv preprint arXiv:1810.05997*, 2018.

Amirata Ghorbani and James Zou. Data shapley: Equitable valuation of data for machine learning. In *International conference on machine learning*, pp. 2242–2251. PMLR, 2019.

Shengbo Gong, Mohammad Hashemi, Juntong Ni, Carl Yang, and Wei Jin. Scalable graph condensation with evolving capabilities. *arXiv preprint arXiv:2502.17614*, 2025.

Will Hamilton, Zhitao Ying, and Jure Leskovec. Inductive representation learning on large graphs. *Advances in neural information processing systems*, 30, 2017.

Shengding Hu, Zheng Xiong, Meng Qu, Xingdi Yuan, Marc-Alexandre Côté, Zhiyuan Liu, and Jian Tang. Graph policy network for transferable active learning on graphs. *Advances in Neural Information Processing Systems*, 33:10174–10185, 2020.

Stefanie Jegelka. Theory of graph neural networks: Representation and learning. *arXiv preprint arXiv:2204.07697*, 2022.

Theis E Jendal, Matteo Lissandrini, Peter Dolog, and Katja Hose. Simple and powerful architecture for inductive recommendation using knowledge graph convolutions. *arXiv preprint arXiv:2209.04185*, 2022.

Junteng Jia and Austin R Benson. Residual correlation in graph neural network regression. In *Proceedings of the 26th ACM SIGKDD international conference on knowledge discovery & data mining*, pp. 588–598, 2020.

Ruoxi Jia, David Dao, Boxin Wang, Frances Ann Hubis, Nezihe Merve Gurel, Bo Li, Ce Zhang, Costas J Spanos, and Dawn Song. Efficient task-specific data valuation for nearest neighbor algorithms. *arXiv preprint arXiv:1908.08619*, 2019.

Wei Jin, Yao Ma, Xiaorui Liu, Xianfeng Tang, Suhang Wang, and Jiliang Tang. Graph structure learning for robust graph neural networks. In *Proceedings of the 26th ACM SIGKDD international conference on knowledge discovery & data mining*, pp. 66–74, 2020.

Wei Jin, Lingxiao Zhao, Shichang Zhang, Yozhen Liu, Jiliang Tang, and Neil Shah. Graph condensation for graph neural networks. *arXiv preprint arXiv:2110.07580*, 2021.

Hoang Anh Just, Feiyang Kang, Jiachen T Wang, Yi Zeng, Myeongseob Ko, Ming Jin, and Ruoxi Jia. Lava: Data valuation without pre-specified learning algorithms. *arXiv preprint arXiv:2305.00054*, 2023.

Thomas N Kipf and Max Welling. Semi-supervised classification with graph convolutional networks. *arXiv preprint arXiv:1609.02907*, 2016.

Yongchan Kwon and James Zou. Beta shapley: a unified and noise-reduced data valuation framework for machine learning. *arXiv preprint arXiv:2110.14049*, 2021.

Yongchan Kwon and James Zou. Data-oob: Out-of-bag estimate as a simple and efficient data value. *arXiv preprint arXiv:2304.07718*, 2023.

Pengyong Li, Jun Wang, Yixuan Qiao, Hao Chen, Yihuan Yu, Xiaojun Yao, Peng Gao, Guotong Xie, and Sen Song. An effective self-supervised framework for learning expressive molecular global representations to drug discovery. *Briefings in Bioinformatics*.

Xin Liu, Mingyu Yan, Lei Deng, Guoqi Li, Xiaochun Ye, and Dongrui Fan. Sampling methods for efficient training of graph convolutional networks: A survey. *IEEE/CAA Journal of Automatica Sinica*, 9(2):205–234, 2021.

Yixin Liu, Yu Zheng, Daokun Zhang, Hongxu Chen, Hao Peng, and Shirui Pan. Towards unsupervised deep graph structure learning. In *Proceedings of the ACM Web Conference 2022*, pp. 1392–1403, 2022a.

Zelei Liu, Yuanyuan Chen, Han Yu, Yang Liu, and Lizhen Cui. Gtg-shapley: Efficient and accurate participant contribution evaluation in federated learning. *ACM Transactions on Intelligent Systems and Technology (TIST)*, 13(4):1–21, 2022b.

Qian Ma, Hongliang Chi, Hengrui Zhang, Kay Liu, Zhiwei Zhang, Lu Cheng, Suhang Wang, Philip S Yu, and Yao Ma. Overcoming pitfalls in graph contrastive learning evaluation: Toward comprehensive benchmarks. *arXiv preprint arXiv:2402.15680*, 2024.

Yao Ma, Xiaorui Liu, Tong Zhao, Yozhen Liu, Jiliang Tang, and Neil Shah. A unified view on graph neural networks as graph signal denoising. In *Proceedings of the 30th ACM international conference on information & knowledge management*, pp. 1202–1211, 2021.

Andrea Mastropietro, Giuseppe Pascoli, Christian Feldmann, Raquel Rodríguez-Pérez, and Jürgen Bajorath. Edgeshaper: Bond-centric shapley value-based explanation method for graph neural networks. *Iscience*, 25(10), 2022.

Dusit Niyato, Athanasios V Vasilakos, and Zhu Kun. Resource and revenue sharing with coalition formation of cloud providers: Game theoretic approach. In *2011 11th IEEE/ACM International Symposium on Cluster, Cloud and Grid Computing*, pp. 215–224. IEEE, 2011.

Ki Nohyun, Hoyong Choi, and Hye Won Chung. Data valuation without training of a model. In *The Eleventh International Conference on Learning Representations*, 2022.

Jian Pei. A survey on data pricing: from economics to data science. *IEEE Transactions on knowledge and Data Engineering*, 34(10):4586–4608, 2020.

Stephanie Schoch, Haifeng Xu, and Yangfeng Ji. Cs-shapley: Class-wise shapley values for data valuation in classification. *Advances in Neural Information Processing Systems*, 35:34574–34585, 2022.

Prithviraj Sen, Galileo Namata, Mustafa Bilgic, Lise Getoor, Brian Galligher, and Tina Eliassi-Rad. Collective classification in network data. *AI magazine*, 29(3):93–93, 2008.

Behrooz Shahsavari and Pieter Abbeel. Short-term traffic forecasting: Modeling and learning spatio-temporal relations in transportation networks using graph neural networks. *University of California at Berkeley, Technical Report No. UCB/EECS-2015-243*, 2015.

Lloyd S Shapley et al. A value for n-person games. 1953.

Oleksandr Shchur, Maximilian Mumme, Aleksandar Bojchevski, and Stephan Günnemann. Pitfalls of graph neural network evaluation. *arXiv preprint arXiv:1811.05868*, 2018.

Rachael Hwee Ling Sim, Xinyi Xu, and Bryan Kian Hsiang Low. Data valuation in machine learning: “ingredients”, strategies, and open challenges. In *Proc. IJCAI*, pp. 5607–5614, 2022.

Shantanu Thakoor, Corentin Tallec, Mohammad Gheshlaghi Azar, Rémi Munos, Petar Veličković, and Michal Valko. Bootstrapped representation learning on graphs. In *ICLR 2021 workshop on geometrical and topological representation learning*, 2021.

Rafaël Van Belle, Charles Van Damme, Hendrik Tytgat, and Jochen De Weerdt. Inductive graph representation learning for fraud detection. *Expert Systems with Applications*, 193:116463, 2022.

Vítor V Vasconcelos, Phillip M Hannam, Simon A Levin, and Jorge M Pacheco. Coalition-structured governance improves cooperation to provide public goods. *Scientific reports*, 10(1):9194, 2020.

Petar Veličković, Guillem Cucurull, Arantxa Casanova, Adriana Romero, Pietro Lio, and Yoshua Bengio. Graph attention networks. *arXiv preprint arXiv:1710.10903*, 2017.

Petar Velickovic, William Fedus, William L Hamilton, Pietro Lio, Yoshua Bengio, and R Devon Hjelm. Deep graph infomax. *ICLR (poster)*, 2(3):4, 2019.

John Von Neumann and Oskar Morgenstern. *Theory of games and economic behavior (60th Anniversary Commemorative Edition)*. Princeton university press, 2007.

Jiachen T Wang and Ruoxi Jia. Data banzhaf: A robust data valuation framework for machine learning. In *International Conference on Artificial Intelligence and Statistics*, pp. 6388–6421. PMLR, 2023.

Yu Wang, Yuying Zhao, Yushun Dong, Huiyuan Chen, Jundong Li, and Tyler Derr. Improving fairness in graph neural networks via mitigating sensitive attribute leakage. In *Proceedings of the 28th ACM SIGKDD conference on knowledge discovery and data mining*, pp. 1938–1948, 2022.

Yu Wang, Kaize Ding, Xiaorui Liu, Jian Kang, Ryan Rossi, and Tyler Derr. Data quality-aware graph machine learning. In *Proceedings of the 33rd ACM International Conference on Information and Knowledge Management*, pp. 5534–5537, 2024.

Eyal Winter. A value for cooperative games with levels structure of cooperation. *International Journal of Game Theory*, 18:227–240, 1989.

Felix Wu, Amauri Souza, Tianyi Zhang, Christopher Fifty, Tao Yu, and Kilian Weinberger. Simplifying graph convolutional networks. In *ICML*. PMLR, 2019.

Haocheng Xia, Jinfei Liu, Jian Lou, Zhan Qin, Kui Ren, Yang Cao, and Li Xiong. Equitable data valuation meets the right to be forgotten in model markets. *Proceedings of the VLDB Endowment*, 16(11):3349–3362, 2023.

Haocheng Xia, Xiang Li, Junyuan Pang, Jinfei Liu, Kui Ren, and Li Xiong. P-shapley: Shapley values on probabilistic classifiers. *Proceedings of the VLDB Endowment*, 17(7):1737–1750, 2024.

Keyulu Xu, Weihua Hu, Jure Leskovec, and Stefanie Jegelka. How powerful are graph neural networks? *arXiv preprint arXiv:1810.00826*, 2018.

Tom Yan and Ariel D Procaccia. If you like shapley then you’ll love the core. In *Proceedings of the AAAI Conference on Artificial Intelligence*, volume 35, pp. 5751–5759, 2021.

Ziyuan Ye, Rihan Huang, Qilin Wu, and Quanying Liu. Same: Uncovering gnn black box with structure-aware shapley-based multipiece explanations. *Advances in Neural Information Processing Systems*, 36, 2024.

Rex Ying, Ruining He, Kaifeng Chen, Pong Eksombatchai, William L Hamilton, and Jure Leskovec. Graph convolutional neural networks for web-scale recommender systems. In *Proceedings of the 24th ACM SIGKDD international conference on knowledge discovery & data mining*, pp. 974–983, 2018.

Jinsung Yoon, Sercan Arik, and Tomas Pfister. Data valuation using reinforcement learning. In *International Conference on Machine Learning*, pp. 10842–10851. PMLR, 2020.

Hao Yuan, Haiyang Yu, Jie Wang, Kang Li, and Shuiwang Ji. On explainability of graph neural networks via subgraph explorations. In *International conference on machine learning*, pp. 12241–12252. PMLR, 2021.

Pu Yuan, Yong Xiao, Guoan Bi, and Liren Zhang. Toward cooperation by carrier aggregation in heterogeneous networks: A hierarchical game approach. *IEEE Transactions on Vehicular Technology*, 66(2):1670–1683, 2016.

Liangliang Zhang, Haoran Bao, and Yao Ma. Extending graph condensation to multi-label datasets: A benchmark study. *arXiv preprint arXiv:2412.17961*, 2024.

Shichang Zhang, Yozen Liu, Yizhou Sun, and Neil Shah. Graph-less neural networks: Teaching old mlps new tricks via distillation. *arXiv preprint arXiv:2110.08727*, 2021a.

Wentao Zhang, Yu Shen, Yang Li, Lei Chen, Zhi Yang, and Bin Cui. Alg: Fast and accurate active learning framework for graph convolutional networks. In *Proceedings of the 2021 international conference on management of data*, pp. 2366–2374, 2021b.

Wentao Zhang, Zhi Yang, Yixin Wang, Yu Shen, Yang Li, Liang Wang, and Bin Cui. Grain: Improving data efficiency of graph neural networks via diversified influence maximization. *arXiv preprint arXiv:2108.00219*, 2021c.

Yifei Zhang, Hao Zhu, Zixing Song, Piotr Koniusz, and Irwin King. Spectral feature augmentation for graph contrastive learning and beyond. In *Proceedings of the AAAI conference on artificial intelligence*, volume 37, pp. 11289–11297, 2023.

Xin Zheng, Yixin Liu, Zhifeng Bao, Meng Fang, Xia Hu, Alan Wee-Chung Liew, and Shirui Pan. Towards data-centric graph machine learning: Review and outlook. *arXiv preprint arXiv:2309.10979*, 2023.

Lina Zhou, Shimei Pan, Jianwu Wang, and Athanasios V Vasilakos. Machine learning on big data: Opportunities and challenges. *Neurocomputing*, 237:350–361, 2017.

Yanqiao Zhu, Yichen Xu, Feng Yu, Qiang Liu, Shu Wu, and Liang Wang. Deep graph contrastive representation learning. *arXiv preprint arXiv:2006.04131*, 2020.

Yaochen Zhu, Jing Ma, Liang Wu, Qi Guo, Liangjie Hong, and Jundong Li. Path-specific counterfactual fairness for recommender systems. In *Proceedings of the 29th ACM SIGKDD Conference on Knowledge Discovery and Data Mining*, pp. 3638–3649, 2023.

A ADDITIONAL RELATED WORK

This section presents an extended review of related works, offering a broader and more nuanced exploration of the literature surrounding Data Valuation and Graph Neural Networks.

A.1 DATA VALUATION

Data Shapley is proposed in (Ghorbani & Zou, 2019) which computes data values with Shapley values in cooperative game theory. Beta Shapley (Kwon & Zou, 2021) is a further generalization of Data Shapley by relaxing the efficiency axiom of the Shapley value. Data Banzhaf (Wang & Jia, 2023) offers a data valuation method which is robust to data noises. Data Valuation with Reinforcement Learning is also explored by (Yoon et al., 2020). KNN-Shapley (Jia et al., 2019) estimates the shapley Value for the K-Nearest Neighbours algorithm in linear time. CS-Shapley (Schoch et al., 2022) provides a new valuation method that differentiate in-class contribution and out-class contribution. Data-OOB (Kwon & Zou, 2023) proposes a data valuation method for a bagging model which leverages the out-of-bag estimate. Just, Hoang Anh, et al (Just et al., 2023) introduce a learning-agnostic data valuation framework by approximating the utility of a dataset according to its class-wise Wasserstein distance. Another training-free data valuation method utilizing the complexity-gap score is proposed at the same time (Nohyun et al., 2022).

However, these methods are primarily designed for traditional i.i.d. data, assuming independence and identical distribution among data points, and are not specifically designed to evaluate graph data. The latter presents higher complexity due to the interconnections and dependencies among individual nodes. P-Shapley (Xia et al., 2024) extends Shapley values by leveraging probabilistic classifier outputs, proposing an alternative utility function that replaces standard accuracy metrics. While this innovation improves valuation accuracy for traditional i.i.d. data, it remains orthogonal to the structural challenges in graph data valuation.

A.2 GRAPH NEURAL NETWORKS

Graph Neural Networks (GNNs) generate informative representations from graph-structured data and facilitate the solving of many graph-related tasks. Bruna et al. (Bruna et al., 2013) first apply the spectral convolution operation to graph-structured data. From the spatial perspective, the spectral convolution can be interpreted to combine the information from its neighbors. GCN (Kipf & Welling, 2016) simplified this spectral convolution and proposed to use first-order approximation. Since then, many other attention-based, sampling-based and simplified GNN variants which follow the same neighborhood aggregation design have been proposed (Veličković et al., 2017; Hamilton et al., 2017; Gasteiger et al., 2018; Wu et al., 2019). Theoretically, those Graph neural networks typically enhance node representations and model expressiveness through a message-passing mechanism, efficiently integrating graph data into the learning of representations (Xu et al., 2018).

A.3 SHAPLEY VALUE IN GRAPH MACHINE LEARNING

The Shapley value has found several applications in graph machine learning, primarily in the domain of explainability for Graph Neural Networks. GraphSVX (Duval & Malliaros, 2021) is one of the early works that utilizes the Shapley value to explain the predictions of GNNs. It identifies influential nodes and features for a particular prediction by treating them as players in a cooperative game. However, GraphSVX focuses on local explanations for individual predictions of a fixed GNN. SubgraphX (Yuan et al., 2021) takes a different approach by explaining GNN predictions through identifying important subgraphs, rather than individual nodes or edges. It uses Monte Carlo tree search to efficiently explore different subgraphs and proposes to use Shapley values as a measure of subgraph importance. EdgeSHAPer (Mastropietro et al., 2022) is another method that assesses edge importance for GNN predictions using the Shapley value concept. It is particularly relevant for molecular graphs where edges represent chemical bonds. GNNShap (Akkas & Azad, 2024) extends upon previous Shapley value based GNN explanation methods by providing explanations for edge, leading to better fidelity scores and faster explanations. SAME (Ye et al., 2024) proposes a structure-aware Shapley-based multipiece explanation method for GNNs that can identify important substructures and provide explanations composed of multiple connected components.

In addition to explainability, Shapley has also been widely adopted for data valuation for conventional machine learning methods as discussed in Section 2. However, it has rarely been utilized for data valuation on graph data. In this work, we pioneer the exploration of graph data valuation, a challenging and previously unexplored problem. Although a recent survey (Zheng et al., 2023) inadvertently refers to GraphSVX as a graph data valuation method, it does not align with the traditional definition of data valuation. We clarify the key differences between graph data valuation (such as our method) and graph explainability (such as GraphSVX) as follows.

1. In general, data valuation (such as our method) aims to understand how graph elements contribute to the model training process, while explainability methods (such as GraphSVX) provide post-hoc explanations for a fixed, pre-trained model.
2. Specifically, our method differs from GraphSVX in several aspects:
 - (a) GraphSVX focuses on the explainability of a local prediction for a single sample, while our method aims to quantify the global contribution of graph elements to the overall model performance.
 - (b) GraphSVX operates post hoc, analyzing the contributions of features and nodes in the *testing graph* to the predictions of an already-trained GNN model, while our approach focuses on the global contribution of each data element in the *training graph* to the GNN model’s training process.
 - (c) GraphSVX employs the standard Shapley value formulation, which assumes free collaboration among players, while our work introduces the PC-Winter value to handle the unique hierarchical coalition structures inherent in graph data valuation.

To the best of our knowledge, our investigation constitutes the first foray into graph data valuation, pioneering research in this previously uncharted domain.

A.4 DATA-CENTRIC LEARNING ON GRAPHS

Data-centric graph learning encompasses various approaches, with data valuation and data-efficient learning sharing similar motivations but distinct methodologies. Data-efficient learning on graphs primarily addresses the challenge of limited labeled data through two main paradigms. Graph self-supervised learning develops rich representations without relying on extensive labels. Within this approach, contrastive methods like Deep Graph Infomax (Velickovic et al., 2019) and GRACE (Zhu et al., 2020) learn by discriminating between different views of the same graph, while more recent non-contrastive techniques including BGRL (Thakoor et al., 2021) and Graph Barlow Twins (Bielak et al., 2022) achieve competitive performance without requiring negative samples. Contemporary research has focused on developing sophisticated feature augmentation strategies Zhang et al. (2023). Chi & Ma (2024) propose enhancing contrastive learning through node similarity metrics, while Ma et al. (2024) establish comprehensive evaluation frameworks. The alternative paradigm, graph active learning, optimizes the selection of nodes for labeling to maximize model performance with minimal annotation effort. Representative approaches include AGE (Cai et al., 2017), which combines multiple selection criteria, GPA (Hu et al., 2020), which reformulates selection as sequential decision-making, and GRAIN (Zhang et al., 2021c), which treat selection as influence maximization problems. More sophisticated techniques have emerged, such as ALG (Zhang et al., 2021b), which balances both representativeness and informativeness, and GALclean (Chi et al., 2024), which addresses active learning challenges in graphs with structural noise. In addition to these data-efficient learning strategies, another key aspect of data-centric graph learning lies in understanding and mitigating biases in GNNs. Fairness-focused studies investigate how GNNs may exhibit biased predictions towards certain demographic subgroups resulted from certain input graph components. For example, recent works have explored to attribute the unfairness exhibited by GNNs to input graph components, such as specific training nodes (Dong et al., 2023), edges (Zhu et al., 2023; Dong et al., 2022a), and subgraphs (Dong et al., 2022b; Wang et al., 2022). Beyond these approaches, data-centric graph learning also encompasses other important branches such as graph structure learning (Jin et al., 2020; Ma et al., 2021; Liu et al., 2022a), which focuses on jointly learning optimal graph structures and node representations; graph condensation (Jin et al., 2021; Zhang et al., 2024; Gong et al., 2025), which aims to distill large-scale graphs into smaller yet information-preserving counterparts for efficient training; and data quality-aware learning (Wang et al., 2024), which develops techniques to identify and mitigate the effects of noisy or corrupted graph data on model performance. In contrast to these approaches that focus on either maximizing performance with limited data or addressing fairness concerns, our work on graph data valuation addresses the fundamental challenge

of quantifying the contributions of graph data elements to model performance through a novel cooperative game-theoretic framework.

B MATHEMATICAL FORMULATION OF WINTER VALUE

The Shapley value offers a solution for equitable payoff distribution in cooperative games, assuming that players cooperate without any predefined structure. In reality, however, cooperative games often have inherent hierarchical coalitions. To accommodate these structured coalitions, the Winter value (Winter, 1989) extends Shapley value to handle this extra coalition constraints.

Specifically, considering level structures \mathcal{B} , with $\mathcal{B} = B_0, \dots, B_n$ representing a sequence of player partitions. Here, a partition, B_m , subdivides the player set \mathcal{P} into a set of disjoint, non-empty subsets T_1, T_2, \dots, T_k . These disjoint subsets satisfy the condition that their union reconstructs the original player set \mathcal{P} , which means $T_1 \cup T_2 \cup \dots \cup T_k = \mathcal{P}$. This partition sequence forms a hierarchy where B_0 represents individual players as the leaves of the structure and B_n functions as the root of this hierarchy.

We then determine $\Omega(\mathcal{B})$, the set of all permissible permutations, starting with a single partition B_m :

$$\Omega(B_m) = \{\pi \in \Pi(\mathcal{P}) : \forall T \in B_m, \forall i, j \in T \text{ and } k \in \mathcal{P}, \\ \text{if } \pi(i) < \pi(k) < \pi(j) \text{ then } k \in T\}.$$

$\Omega(\mathcal{B})$ can be further defined as the set of permutations which satisfy all constraints of all levels, $\Omega(\mathcal{B}) = \bigcap_{t=0}^n \Omega(B_t)$.

A permissible permutation π from the set $\Omega(\mathcal{B})$ requires that players from any derived coalition of \mathcal{B} must appear consecutively. Given the defined set of permissible permutations $\Omega(\mathcal{B})$, the Winter value Φ for player i is calculated as:

$$\Phi_i(\mathcal{P}, U, \mathcal{B}) = \frac{1}{|\Omega(\mathcal{B})|} \sum_{\pi \in \Omega(\mathcal{B})} (U(\mathcal{P}_i^\pi \cup i) - U(\mathcal{P}_i^\pi))$$

where $\mathcal{P}_i^\pi = \{j \in N : \pi(j) < \pi(i)\}$ is the set of predecessors of i at the permutation σ and U is the utility function in the cooperative game.

C PROOFS OF THEOREMS

Theorem 1 (Specificity). *Given a contribution tree \mathcal{T} with a set of players \mathcal{P} , any DFS traversal over the \mathcal{T} results in a permissible permutation of \mathcal{P} that satisfies both the Level Constraint and Precedence Constraint.*

Proof. We validate the theorem by demonstrating that a permutation obtained through pre-order traversal on \mathcal{T} meets Level Constraints and Precedence Constraints. (1) Level Constraints: During a pre-order traversal of \mathcal{T} , a node p and its descendants $\mathcal{D}(p)$ are visited sequentially before moving to another subtree. Thus, in the resulting permutation π , the positions of p and any $i, j \in \mathcal{D}(p)$ are inherently close to each other, satisfying the condition $|\pi[i] - \pi[j]| \leq |\mathcal{D}(p)|$. This contiguous traversal ensures that all descendants and the node itself form a continuous sequence in π , meeting the Level Constraint. (2) Precedence Constraints: In the same traversal, each node p is visited before its descendants. Therefore, in π , the position of p always precedes the positions of its descendants, i.e., $\pi[p] < \pi[i]$ for all $i \in \mathcal{D}(p)$. This traversal pattern naturally embeds the hierarchy of the tree into the permutation, ensuring that ancestors are positioned before their descendants, in line with the Precedence Constraint. \square

Theorem 2 (Exhaustiveness). *Given a contribution tree \mathcal{T} with a set of players \mathcal{P} , any permissible permutation $\pi \in \Omega$ can be generated by a corresponding DFS traversal of \mathcal{T} .*

Proof. To prove the theorem of exhaustiveness, consider a contribution tree \mathcal{T} with a set of players \mathcal{P} and any permissible permutation $\pi \in \Omega$. We apply induction on the depth of \mathcal{T} . For the base case, when \mathcal{T} has a depth of 1, which means there are no dependencies among players, any permissible

permutation of players is trivially generated by a DFS traversal since there are no constraints on the order of traversal. For the inductive step, assume the theorem holds for contribution trees of depth k . For a contribution tree of depth $k + 1$ \mathcal{T}^{k+1} , consider its root node and subtrees of depth k rooted at the child nodes of the root node. For any given permissible permutation π corresponding to the \mathcal{T}^{k+1} , according to the Level Constraint, it is a direct composition of the permissible permutations corresponding to the subtrees of depth k rooted at the child nodes of the root node. Now we can construct a DFS traversal over the contribution tree \mathcal{T}^{k+1} that can generate π . Specifically, the order of composition defines the traversal order of the child nodes of the root node. Furthermore, by the inductive hypothesis, any permissible permutations corresponding to the subtrees can be generated by DFS traversal over the subtrees. Hence, at each child node of the root node, we just follow the corresponding DFS traversal of its corresponding tree. This DFS traversal can generate the given permutation π , which completes the proof. \square

D HIERARCHICAL TRUNCATION

In Table 1, we present data comparing the number of model re-trainings on the all six dataset with and without the application of truncation. For the Citeseer dataset, the truncation ratios are defined as 1st-hop: 0.5 and 2nd-hop: 0.7. For the remaining datasets, the truncation ratios are set at 1st-hop: 0.7 and 2nd-hop: 0.9. The results clearly indicate that the number of model re-trainings is substantially reduced when truncation is applied. For instance, focusing on the Citeseer dataset the application of truncation significantly reduces the number of retrainings from 1388 to 535. This significant decrease, especially in larger datasets like Amazon-Photo and Amazon-Computer, where retraining instances decrease from 147664 to 6258 and from 317959 to 12139 respectively, can be attributed to the substantial number of 2-distance neighbors present in these datasets. The application of truncation effectively reduces the computation by omitting a considerable portion of these neighbors. This finding also implies that overall training time is decreased while still maintaining the ability to accurately measure the total marginal contribution.

Table 1: Retraining Number Comparison Per Permutation

Dataset	w.o. Truncation	w.t. Truncation
Cora	2241	756
Citeseer	1388	535
Pubmed	3683	887
Amazon-Photo	147664	6258
Amazon-Computer	317959	12139
Coauthor-Physics	11178	852

E MIXED NODE DROPPING EXPERIMENT

As mentioned in the experiment, labeled nodes will dominate the performance curve when both labeled nodes and unlabeled nodes. The corresponding experiment result is shown in the Figure 6. This experiment validates the assumption that a effective data valuation method would naturally rank labeled nodes for earlier removal over their unlabeled counterparts. For instance, in the Cora dataset, we can observe that the initial drop in accuracy is significant, indicating the removal of high-value labeled nodes. As the experiment progresses and more nodes are removed, the accuracy barely changes, reflecting the removal of unlabeled nodes which has a minimal impact on performance when most labeled nodes are unavailable. The observed pattern across all datasets is consistent: there is a substantial drop in performance at the beginning, followed by a plateau with minimal changes. This suggests that the initial set of nodes removed, predominantly high-value labeled nodes, are those critical to the model’s performance, whereas the subsequent nodes show less influence on the outcome.

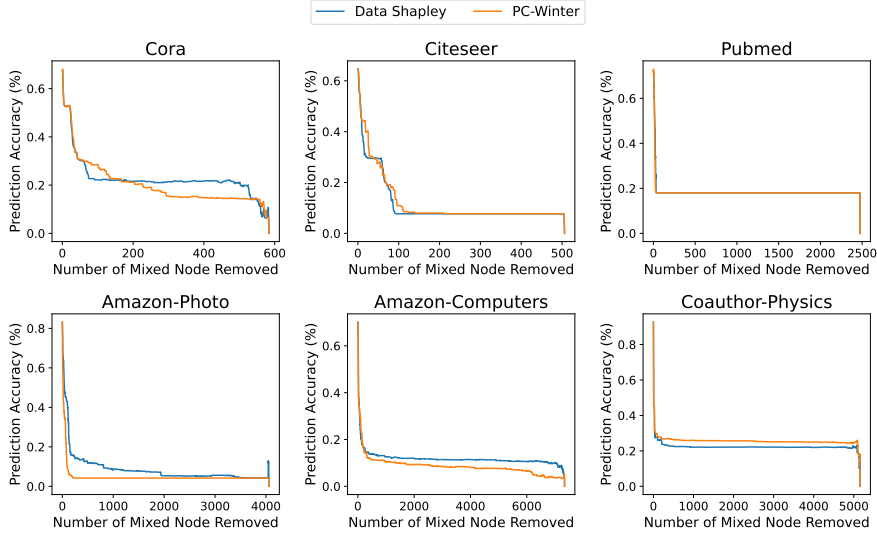


Figure 6: Mixed Node Dropping Experiment

F LABELED NODE DROPPING EXPERIMENT

Here, we perform node dropping experiment employing the aggregated value define in the main-body of paper, to demonstrate that PC-Winter can capture the heterogeneous influence of labeled nodes. As shown in the Figure 7, both PC-Winter and Data Shapley demonstrate effectiveness in capturing the diverse contributions of labeled nodes to the model’s performance. Particularly in the Pubmed and Amazon-Photo datasets, PC-Winter exhibits better performance compared to Data Shapley. In other datasets, such as Cora, Citeseer, and Coauthor-Physics, PC-Winter shows results that are on par with Data Shapley.

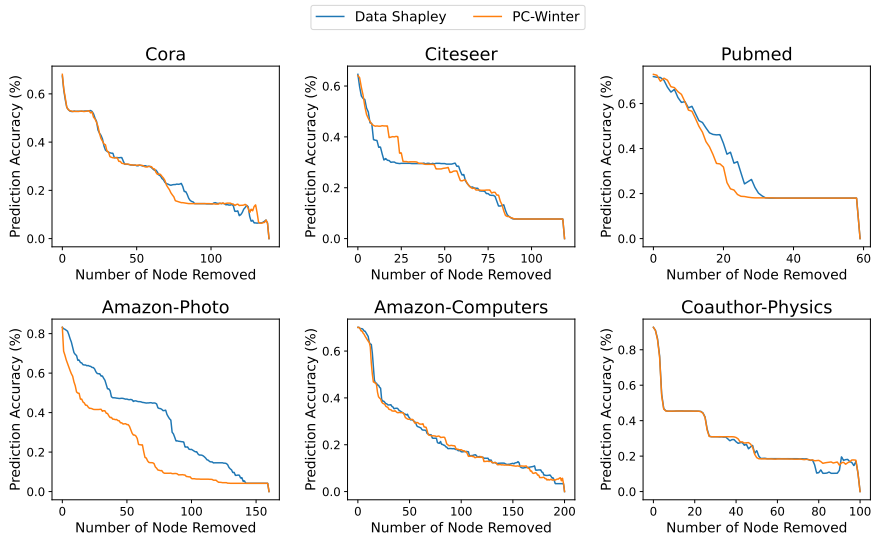


Figure 7: Labeled Node Dropping Experiment

G EXPERIMENTAL DETAILS

G.1 INDUCTIVE SETTING

Our experiments focus on the inductive node classification task, which aims to generalize a trained model to unseen nodes and is commonly adopted in real-world graph applications (Hamilton et al., 2017; Van Belle et al., 2022; Jendal et al., 2022; D’Amico et al., 2023). Unlike the transductive setting (Kipf & Welling, 2016) which incorporates the test nodes in the model training process, the inductive setting separates them apart from the training graph. Such a separation allows us to measure the value of the graph elements in the training graph solely based on their contribution to GNN model training. Following (Hamilton et al., 2017), we split each graph \mathcal{G} into 3 disjoint subgraphs: training graph \mathcal{G}_{tr} , validation graph \mathcal{G}_{va} , and test graph \mathcal{G}_{te} . The training graph \mathcal{G}_{tr} is constructed without any nodes from the validation or test set. Correspondingly, edges connecting to a validation node or a testing node are also removed from the training graph. For the validation graph \mathcal{V}_{va} and the testing graph \mathcal{V}_{te} , only edges with both nodes within the respective node sets are retained, which is aligned with the inductive setting in prior work (Zhang et al., 2021a). We utilize \mathcal{G}_{tr} to train the GNN model, which is evaluated on \mathcal{V}_{va} for obtaining the data values for elements. The test graph \mathcal{V}_{te} is utilized to evaluate the effectiveness of the obtained values.

G.2 DATASETS

We assess the proposed approach on six real-world benchmark datasets. These include three citation graphs, Cora, Citeseer and Pubmed (Sen et al., 2008) and two Amazon Datasets, Amazon-Photo and Amazon-Computer, and Coauthor-Physics (Shchur et al., 2018). The detailed statistics of datasets are summarized in Table 2.

The statistics presented in Table 2 characterize both the structural properties and experimental settings of each dataset. The first four columns present basic graph statistics: the total number of nodes (# Node), edges (# Edge), classes (# Class), and node feature dimensions (# Feature). These statistics together provide a comprehensive view of each dataset’s scale and complexity. The last column (# Train/Val/Test) specifies our experimental setup following the inductive learning setting, where we split the nodes into three mutually exclusive sets: training, validation, and testing nodes. For example, in the Cora dataset (140/500/1,000), we select 140 nodes for training, 500 for validation, and 1,000 for testing. The training graph \mathcal{G}_{tr} is constructed using only training nodes and their 2-hop neighbors, explicitly excluding any validation or testing nodes. Separate subgraphs \mathcal{G}_{va} and \mathcal{G}_{te} are created using only validation and testing nodes respectively, maintaining strict separation between splits. This inductive setting ensures no information leakage between splits, as the graph elements (nodes and edges) are mutually exclusive between training, validation, and testing graphs. A detailed visualization of this split setting can be found in Section M, which illustrates both the inductive graph split and the PC-Winter value estimation procedure.

Table 2: Dataset Summary

Dataset	# Node	# Edge	# Class	# Feature	# Train/Val/Test
Cora	2,708	5,429	7	1,433	140 / 500 / 1,000
Citeseer	3,327	4,732	6	3,703	120 / 500 / 1,000
Pubmed	19,717	44,338	3	500	60 / 500 / 1,000
Amazon-Photo	7,650	119,081	8	745	160 / 20% / 20%
Amazon-Computer	13,752	245,861	10	767	200 / 20% / 20%
Coauthor-Physics	34,493	247,962	8	745	100 / 20% / 20%

G.3 DATASET SPLIT

In the conducted experiments, we split each graph \mathcal{G} into 3 disjoint subgraphs: training graph \mathcal{G}_{tr} , validation graph \mathcal{G}_{va} , and test graph \mathcal{G}_{te} . The training graph \mathcal{G}_{tr} is constructed without any nodes from the validation or test set. Correspondingly, edges connecting to a validation node or a testing node are also removed from the training graph. For the validation graph \mathcal{V}_{va} and the testing graph \mathcal{V}_{te} , only edges with both nodes within the respective node sets are retained, which is aligned with

the inductive setting in prior work (Zhang et al., 2021a). We utilize \mathcal{G}_{tr} to train the GNN model, which is evaluated on \mathcal{V}_{va} for obtaining the data values for elements. The test graph \mathcal{V}_{te} is utilized to evaluate the effectiveness of the obtained values. In the case of the specific split for each dataset, for the citation networks, we adopt public train/val/test splits in our experiments. For the remaining datasets, we randomly select 20 labeled nodes per class for training, 20% nodes for validation and 20% nodes as the testing set.

G.4 CONVERGENCE CRITERIA

Convergence Criterion. For permutation-based data valuation methods such as Data Shapley and PC-Winter, we follow convergence criteria similar to the one applied in prior work (Ghorbani & Zou, 2019) to determine the number of permutations for approximating data values:

$$\frac{1}{n} \sum_{i=1}^n \frac{|v_i^t - v_i^{t-20}|}{|v_i^t|} < 0.05$$

where v_i^t is the estimated value for the data element i using the first t sampled permutations.

Time Limit. For larger datasets, sampling a sufficient number of permutations for converged data values could be impractical in time. To address this and to stay within a realistic scope, we cap the computation time at 120 GPU hours on NVIDIA Titan RTX, after which the calculation is terminated.

G.5 TRUNCATION RATIOS AND HYPER-PARAMETERS

Table 3 includes the hyper-parameters and truncation ratios used for value estimation.

Table 3: Truncation Ratios and Hyper-parameters

Dataset	Truncation Ratio	Learning Rate	Epoch	Weight Decay
Cora	0.5-0.7	0.01	200	5e-4
Citeseer	0.5-0.7	0.01	200	5e-4
Pubmed	0.5-0.7	0.01	200	5e-4
Amazon-Photo	0.7-0.9	0.1	200	0
Amazon-Computer	0.7-0.9	0.1	200	0
Coauthor-Physics	0.7-0.9	0.01	30	5e-4

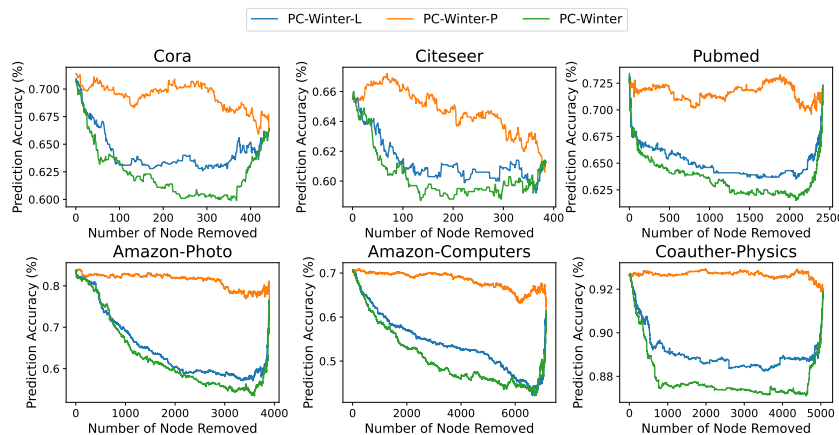


Figure 8: Ablation Study

G.6 BASELINES

G.6.1 DROPPING HIGH-VALUE NODES

Here, we introduce the baselines used for comparison to validate the effectiveness of the proposed method in the dropping node experiment:

- **Random Value:** It assigns nodes with random values, which leads to random ranking without any specific pattern or correlation to the node’s features.
- **Degree-based Value:** A node is assigned its degree as its value, assuming that a node’s importance in the graph is indicated by its degree.
- **Leave-one-out (LOO):** This method calculates a node’s value based on its marginal contribution compared to the rest of the training nodes. Specifically, the value $v(i)$ assigned to each node i is its marginal utility, calculated as $v(i) = U(\mathcal{G}_{tr}) - U(\mathcal{G}_{tr}^{-i})$, where \mathcal{G}_{tr}^{-i} denotes the training graph excluding node i . The utility function U measures the model’s validation performance when trained on the given graph. In essence, the drop in performance due to the removal of a node is treated as the value of that node.
- **Data Shapley:** The node values are approximated with the Monte Carlo sampling method of Data Shapley (Ghorbani & Zou, 2019) by treating both labeled nodes and unlabeled nodes as players. Notably, we only include those unlabeled nodes within the 2-hop neighbors of labeled nodes in the evaluation process. There are two approximation methods: Truncated Monte Carlo approximation and Gradient Shapley in (Ghorbani & Zou, 2019). We adopt the Truncated Monte Carlo approximation as it consistently outperforms the other variants in various experiments.

Notably, there is a recent work (Chen et al., 2022) that aims at characterizing the impact of elements on model performance. Their goal is to approximate LOO value. Thus, we do not include it as a baseline as LOO is already included.

G.6.2 ADDING HIGH-VALUE EDGES

Here are the detailed descriptions on the baselines applied in the edge adding experiment.

- **Random Value:** it assigns edges with random values, reflecting a baseline where no information are used for differentiating the importance of edges.
- **Edge-Betweenness:** the Edge-Betweenness of an edge e is the fraction of all pairwise shortest paths that go through e . This classic approach assesses an edge’s importance based on its role in the overall network connectivity.
- **Leave-one-out (LOO):** This method calculates a edge e ’s value $v(e)$ based on its marginal contribution compared to the rest of the training graph. In specific, $v(e) = U(\mathcal{G}_{tr}) - U(\mathcal{G}_{tr}^{-e})$ Here, $e \in \mathcal{G}_{tr}$ represents an edge in the training graph \mathcal{G}_{tr} , and \mathcal{G}_{tr}^{-e} refers to the training graph excluding the edge e .

H DETAILED QUANTITATIVE RESULTS

This appendix presents detailed quantitative results for the node dropping and edge addition experiments discussed in the main text. To provide a more rigorous evaluation of our method’s effectiveness, we introduce four key metrics that quantify the insights from Figures 3 and 4 in the main text:

For the node dropping experiment:

- **Minimum Accuracy:** The lowest accuracy reached during node removal.
- **Mean Accuracy:** The average accuracy across all node removal steps.

For the edge addition experiment:

- **Maximum Accuracy:** The highest accuracy reached during edge addition.
- **Mean Accuracy:** The average accuracy across all edge addition steps.

The rationale behind these metrics is as follows: (1) For node dropping, the Minimum Accuracy refers to the lowest accuracy reached during node removal. A lower value for this metric indicates better

identification of the most critical nodes, whose removal causes the largest performance drop. This metric is designed to capture the method’s ability to identify the most influential nodes in the graph. Similarly, the Mean Accuracy measures the average accuracy across all node removal steps. A lower mean accuracy suggests the method consistently identifies important nodes throughout the removal process, maintaining lower performance overall. This reflects the method’s ability to consistently pinpoint valuable nodes across different stages of the removal process. (2) For edge addition, the Maximum Accuracy corresponds to the highest accuracy achieved during edge addition. A higher value for this metric signals better identification of the most valuable edges, whose addition results in the largest performance improvement. This metric captures the method’s capacity to identify edges that significantly enhance the graph’s information content. The Mean Accuracy measures the average accuracy across all edge addition steps, with a higher mean accuracy suggesting that the method consistently identifies important edges throughout the process, maintaining higher performance overall. This reflects the method’s ability to recognize valuable edges across different stages of the addition process. These metrics allow us to quantitatively assess each method’s effectiveness in identifying high-value graph elements. They provide concrete measures of how well each method causes the accuracy curve to drop deeply and consistently in node dropping experiments, and how quickly and sustainedly it raises the accuracy curve in edge addition experiments.

Tables 4 and 5 show the minimum and mean accuracies for the node dropping experiment, while Tables 6 and 7 present the maximum and mean accuracies for the edge addition experiment. These results provide a comprehensive quantitative basis for evaluating the performance of our **PC-Winter** method compared to other baselines across various graph datasets.

Table 4: Node Dropping - Minimum Accuracy

Method	Cora	Citeseer	Pubmed	Amazon-Photo	Amazon-Computers	Coauthor-Physics
Random	0.6600	0.6130	0.7110	0.7176	0.5676	0.9164
Degree	0.6600	0.6040	0.6990	0.6752	0.5625	0.9135
LOO	0.6580	0.6130	0.6920	0.6778	0.5582	0.9039
Data Shapley	0.6200	0.5910	0.6230	0.6255	0.4891	0.8863
PC-Winter	0.5990	0.5870	0.6150	0.5340	0.4207	0.8710

Table 5: Node Dropping - Mean Accuracy

Method	Cora	Citeseer	Pubmed	Amazon-Photo	Amazon-Computers	Coauthor-Physics
Random	0.6903	0.6411	0.7294	0.8140	0.6807	0.9249
Degree	0.6814	0.6354	0.7156	0.7377	0.6637	0.9215
LOO	0.6832	0.6349	0.7020	0.7296	0.6012	0.9197
Data Shapley	0.6421	0.6124	0.6437	0.7049	0.5467	0.8988
PC-Winter	0.6248	0.6034	0.6362	0.6306	0.5075	0.8793

Table 6: Edge Addition - Maximum Accuracy

Method	Cora	Citeseer	Pubmed	Amazon-Photo	Amazon-Computers	Coauthor-Physics
Random	0.7160	0.6550	0.7410	0.8621	0.7975	0.9266
Edge Betweenness	0.7220	0.6630	0.7470	0.8791	0.7996	0.9255
LOO	0.7140	0.6610	0.7350	0.8582	0.7953	0.9243
PC-Winter	0.7310	0.6750	0.7600	0.8739	0.8145	0.9297

The results in Tables 4 and 5 demonstrate that **PC-Winter** consistently achieves the lowest minimum and mean accuracies across all datasets in the node dropping experiment. This indicates that **PC-Winter** is more effective at identifying critical nodes whose removal significantly impacts model performance. The performance gap is particularly notable in larger and more complex datasets such as Amazon-Photo and Amazon-Computers.

For the edge addition experiment, Tables 6 and 7 show that **PC-Winter** achieves the highest maximum and mean accuracies across all datasets. This suggests that **PC-Winter** is superior at identifying valuable edges whose addition leads to the most significant performance improvements. The advantage of **PC-Winter** is consistent across different graph structures and sizes, from smaller networks like Cora to larger ones like Coauthor-Physics.

Table 7: Edge Addition - Mean Accuracy

Method	Cora	Citeseer	Pubmed	Amazon-Photo	Amazon-Computers	Coauthor-Physics
Random	0.6894	0.6330	0.7227	0.8438	0.7823	0.9226
Edge Betweenness	0.6855	0.6217	0.7287	0.8475	0.7752	0.9202
LOO	0.6809	0.6339	0.7146	0.8452	0.7599	0.9186
PC-Winter	0.7197	0.6616	0.7511	0.8640	0.8023	0.9266

These quantitative results corroborate the visual trends observed in Figures 3 and 4 of the main text. They provide strong evidence for the effectiveness of PC-Winter in both identifying critical nodes for removal and valuable edges for addition, outperforming other baseline methods across various graph datasets.

I ABLATION STUDY AND PARAMETER ANALYSIS

I.1 ABLATION STUDY

This Appendix Section offers an in-depth ablation analysis across full six datasets to investigates the necessity of both Level Constraint and Precedence Constraint in defining an effective graph value. The results, as shown in Figure 8, consistently demonstrate across all datasets that the absence of either constraint leads to a degraded result when compared to the one incorporating both. This underscores the importance of both two constraints in capturing the contributions of graph elements to overall model performance.

I.2 THE IMPACT OF PERMUTATION NUMBER

This part expands upon the permutation analysis presented in the main paper. It provides comprehensive results across various datasets, illustrating how different numbers of sample permutations impact the accuracy of PC-Winter. The results of full datasets are shown in Figure 9. The results reveals

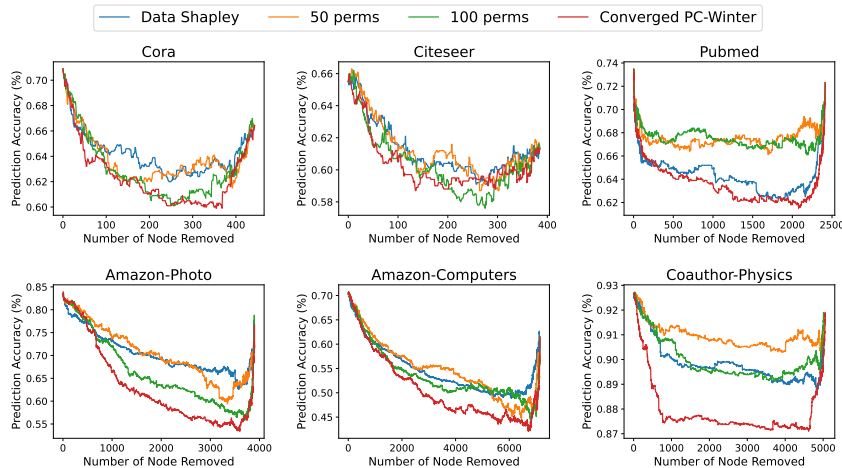


Figure 9: The Impact of Permutation Numbers

that increasing the number of permutations generally improves the performance and accuracy of the valuation. PC-Winter also show robust results even with a limited number of permutations, highlighting its effectiveness. The phenomenon is consistent across all datasets where our approach with just 50 to 100 permutations manages to compete closely with the fully converged Data Shapley, emphasizing the efficiency of PC-Winter in various settings.

I.3 THE IMPACT OF TRUNCATION RATIOS

Our approach involves truncating the iterations involving the first and second-hop neighbors of a labeled node during value estimation. Here, we investigate the impact of truncation proportion on overall performance, using the same number of permutations as in our primary node-dropping experiment. As shown in Figure 10, we adjusted the truncation ratios for the Citation Network datasets. The ratios ranged from truncating 50% of the first-hop and 70% of the second-hop neighbors (0.5-0.7), up to 90% truncation for either first-hop (0.9-0.7) or second-hop (0.5-0.9) neighbors. For the Cora and Citeseer datasets, increasing truncation at the first-hop level had a minimal impact on performance, and PC-Winter still significantly outperformed Data Shapley. In the case of the Pubmed dataset, more extensive truncation at the first-hop level notably reduced performance. Regarding large datasets such as the Amazon, while truncation at either the first or second-hop levels had a marginal negative effect on performance, PC-Winter’s estimated data values generally remained superior to results of Data Shapley.

In addition, we provide a detailed analysis of our truncation strategy across other datasets. It includes results not presented in the main text, focusing on the impact of limiting model retraining times to the first and second-hop neighbors in value estimation. We investigate the impact of truncation proportion on overall performance, using the same number of permutations as in our primary node-dropping experiment. The findings on full datasets are illustrated in Figure 10. Specifically, our findings reveal that in datasets like Cora and Citeseer, adjusting truncation primarily at the first-hop level has a negligible impact on the accuracy of node valuation, with PC-Winter still maintaining a considerable advantage over Data Shapley. For large datasets such as the Amazon-Photo, Amazon-Computers and Coauthor-Physics, while truncations had a marginal negative effect on performance, PC-Winter’s estimated data values generally remained better than Data Shapley. This analysis indicates that PC-Winter can afford to employ larger truncation, enhancing computational efficiency without substantially sacrificing the quality of data valuation.

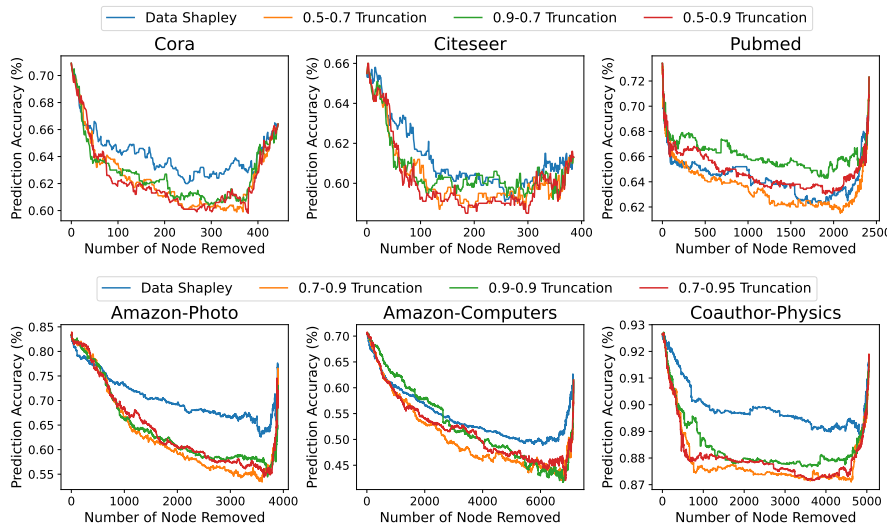


Figure 10: The Impact of Truncation Ratios

Table 8: Permutation Number and Time Comparison

Dataset	Truncation	PC-Winter		Data Shapley	
		Perm Number	Perm Time (hrs)	Perm Number	Perm Time (hrs)
Cora	0.5-0.7	325	0.013	327	0.024
Citeseer	0.5-0.7	291	0.018	279	0.037
Pubmed	0.5-0.7	316	0.025	281	0.285
Amazon-Photo	0.7-0.9	418	0.211	109	1.105
Amazon-Computer	0.7-0.9	181	0.662	33	3.566
Coauthor-Physics	0.7-0.9	460	0.119	45	2.642

I.4 EFFICIENCY ANALYSIS

Here, we compare the computational efficiency of our proposed method PC-Winter and the Data Shapley approach in terms of permutation number and time per permutation. As detailed in Table 8, the results indicate that PC-Winter requires significantly less time to compute each permutation across various datasets. Specifically, for the Cora dataset, PC-Winter completes each permutation in approximately half the time required by Data Shapley. Moving to larger datasets, the efficiency of PC-Winter becomes even more pronounced. For instance, in the Amazon-Computer dataset, PC-Winter’s permutation time is only a fraction of what is required by Data Shapley —PC-Winter takes slightly over half an hour per permutation whereas Data Shapley exceeds three and a half hours. This consistent reduction in permutation time demonstrates the computational advantage of PC-Winter, particularly when handling large graphs. Combining the insights from the Permutation Analysis shown in Figure 9 with the Permutation Comparison Table 8, we observe that for datasets such as Cora, Citeseer, Amazon-Photo, and Amazon-Computer, around 50 permutations are sufficient for PC-Winter to achieve performance comparable to that of Data Shapley. Simple calculations demonstrate that our method is significantly faster than Data Shapley in achieving similar performance levels. For instance, in the Cora dataset, the speedup factor is $\frac{327 \times 0.024}{50 \times 0.013} = 12.07$, and for the Citeseer dataset, it is $\frac{279 \times 0.037}{50 \times 0.018} = 11.47$. The speedup factors for Amazon-Photo and Amazon-Computer are $\frac{109 \times 1.105}{50 \times 0.211} = 11.42$, and $\frac{33 \times 3.566}{50 \times 0.662} = 3.57$, respectively. For Coauthor-Physics, it takes about 100 permutations for PC-Winter to match the performance of Data Shapley, which implies a speedup factor of $\frac{45 \times 2.642}{100 \times 0.119} = 10.00$. In conclusion, PC-Winter can achieve stronger performance than Data Shapley using the same or even less time. Furthermore, it takes PC-Winter much less time to achieve comparable performance as Data Shapley. Notably, though PC-Winter is significantly more efficient than Data Shapley, its scalability is still limited, and future work in further improving its efficiency is desired.

I.5 COMPLEXITY ANALYSIS

We analyze the complexity of the PC-Winter. For convenience, we assume that we are dealing with a d -regular graph. There are a total of L labeled nodes in the graph. As described in the paper, we deal with a GNN model with 2 layers. Without loss of generality, we use F to denote the dimensionality of node representations in each layer. We assume the number of classes in the dataset is C . For hierarchical truncation, we assume we adopt a truncation ratio of $r_1 - r_2$, which is consistent with the description in Section 3.4. Then, the number of nodes in a computation tree for any labeled node is $N_{full} = 1 + d + d^2$. With hierarchical truncation, the number of nodes in the truncated computation tree is $N_{trun} = 1 + d \cdot (1 - r_1) + d^2 \cdot (1 - r_1)(1 - r_2)$. When the truncation ratios are large, $N_{trun} \ll N_{full}$. For instance, when $r_1 = r_2 = 0.9$, N_{trun} could be less than 5Time Complexity Analysis: We now analyze the time complexity of a single permissible permutation of the PC-Winter algorithm. We begin by examining the time complexity of generating a single permissible permutation. Then, we investigate the complexity of a single model retraining and provide the total retraining number for a single permutation. Finally, we combine these analyses to derive the overall time complexity for generating one permissible permutation and going through it for calculating the marginal contributions. Time complexity of generating a single permissible permutation: The time complexity of traversing the truncated contribution tree to generate a single permissible permutation is $O(L \cdot N_{trun})$. In particular, there are $L \cdot N_{trun} + 1$ nodes in the contribution tree (including the dummy node). Hence, the cost of a DFS traversal over the contribution tree is

$O(L \cdot N_{\text{trun}} + 1 + L \cdot N_{\text{trun}}) = O(L \cdot N_{\text{trun}})$. Time complexity of one model retraining: As described in Section 3.4, with local propagation, for each model retraining, we only need to perform feature aggregation on a single partial computation tree. The size of a partial computation tree is, on average, $\frac{N_{\text{trun}}}{2}$. Therefore, the feature aggregation complexity for each retraining step is $O(\frac{N_{\text{trun}}}{2} \cdot F)$, where F is the dimension of node features. The feature transformation complexity for each model retraining is $O(F \cdot F + F \cdot C) = O(F^2)$, where C is the output dimension (number of classes) of the GNN model. Therefore, the total time complexity of a single retraining is $O(\frac{N_{\text{trun}}}{2} \cdot F + F^2)$. Without local propagation, the feature aggregation complexity for each model retraining would be much larger, since the propagation needs to be performed on the entire graph. The number of model retrainings in a single permutation: In a permissible permutation, we need to perform retraining for each node in the truncated contribution tree, which has $L \cdot N_{\text{trun}}$ nodes in total. Therefore, $L \cdot N_{\text{trun}}$ model retrainings are needed for a single permutation. Total time complexity for a single permissible permutation: With local propagation and hierarchical truncation, the total time complexity of a single permissible permutation in PC-Winter is: $O(L \cdot N_{\text{trun}} + L \cdot N_{\text{trun}} \cdot (\frac{N_{\text{trun}}}{2} \cdot F + F^2)) = O(L \cdot N_{\text{trun}} \cdot (1 + \frac{N_{\text{trun}}}{2} \cdot F + F^2)) = O(L \cdot N_{\text{trun}} \cdot (\frac{N_{\text{trun}}}{2} \cdot F + F^2))$. Notably, the time complexity of generating a permissible permutation is negligible compared to the cost of model retraining. The proposed strategies, hierarchical truncation, and local propagation, help reduce the overall time complexity of the PC-Winter algorithm. In particular, hierarchical truncation makes N_{trun} much smaller than N_{full} , greatly decreasing the total number of model retraining required for a single permutation. On the other hand, Local propagation reduces the feature aggregation complexity, greatly reducing the cost of each retraining.

The proposed strategies, hierarchical truncation, and local propagation, help reduce the overall time complexity of the PC-Winter algorithm. In particular, hierarchical truncation makes N_{trun} much smaller than N_{full} , greatly decreasing the total number of model retraining required for a single permutation. On the other hand, Local propagation reduces the feature aggregation complexity, greatly reducing the cost of each retraining.

It is worth noting that, similar to traditional Shapley value computation and its variants such as S-Shapley, computing the exact PC-Winter value remains $\#P$ -complete (Xia et al., 2023). Our analysis above specifically describes the time complexity of our approximation framework, which achieves polynomial-time efficiency through Monte Carlo permutation sampling, hierarchical truncation, and local propagation. This approach is aligned with the polynomial-time permutation-based approximation methods in the literature (Xia et al., 2023).

J ADDITIONAL REGRESSION TASK EVALUATION

To validate our method’s effectiveness beyond classification tasks, we conducted additional experiments on node regression using the US election 2012 dataset from (Jia & Benson, 2020). We employed a 2-layer SGC model in an inductive setting, sampling 30% of nodes in the training graph as labeled nodes.

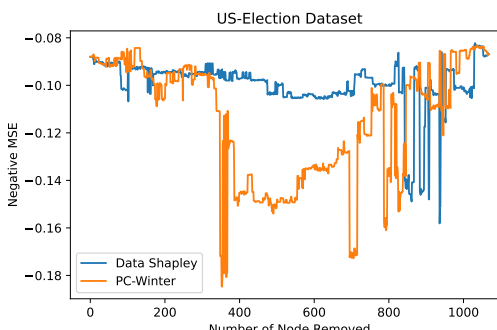


Figure 11: Comparison of PC-Winter and Data Shapley on node regression task. The y-axis shows negative MSE (higher is better) as nodes are progressively removed based on their computed values.

For rigorous comparison, we configured both PC-Winter and Data Shapley under consistent experimental settings. PC-Winter was implemented with a truncation ratio of 0.5-0.7, while both methods used 50 permutations for value computation. The evaluation protocol involved dropping unlabeled training nodes sequentially based on their computed values, from most to least important, to assess each method’s ability to identify influential nodes.

We evaluated performance using negative MSE, calculated as the negative of the mean squared error between predicted and actual values. This metric choice serves dual purposes - it maintains consistency with our classification experiments where higher values indicate better performance, while enabling direct interpretation of performance drops. When removing crucial nodes, we expect to see a decline in negative MSE, with steeper declines indicating better identification of important nodes.

Figure 11 shows the comparative results between PC-Winter and Data Shapley. PC-Winter achieves a better mean negative MSE of -0.1147 compared to Data Shapley’s -0.0993. The steeper drops in PC-Winter’s curve demonstrate its superior ability to identify nodes crucial for model performance. This performance advantage remains consistent across different stages of node removal, indicating robust valuation quality throughout the evaluation process.

This regression task evaluation strengthens our original findings in several significant ways. First, it validates our method’s effectiveness on continuous-valued predictions, extending beyond the discrete classification setting. Second, the inductive setup tests the method’s generalization capability. Third, the successful application with an SGC architecture demonstrates robustness across different model types. Together with our classification results, this comprehensive evaluation provides compelling evidence for both the effectiveness and generality of our approach in graph data valuation.

K CLASS-BALANCED ACCURACY ANALYSIS

To provide a more comprehensive evaluation perspective, we analyze PC-Winter’s performance using class-balanced accuracy. This metric helps assess whether our method can effectively identify important nodes across all classes without bias. Class-balanced accuracy is particularly important for datasets with imbalanced class distributions, as it gives equal weight to each class regardless of its size.

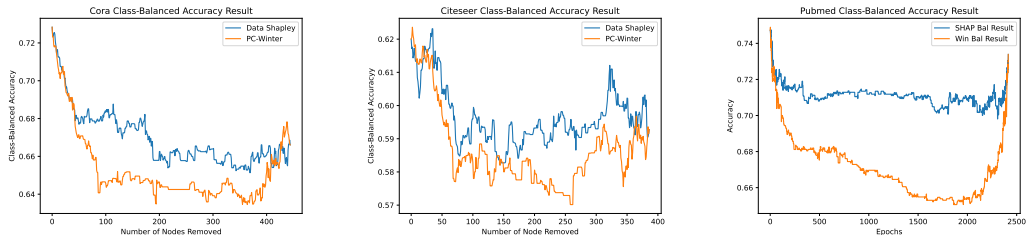


Figure 12: Class-balanced accuracy comparison between PC-Winter and Data Shapley across different datasets. The x-axis shows the number of nodes removed, and the y-axis shows the class-balanced accuracy. From left to right: (a) Cora, (b) Citeseer, (c) Pubmed.

Figure 12 presents the comparison between PC-Winter and Data Shapley using class-balanced accuracy on three benchmark datasets. On the Cora dataset, PC-Winter demonstrates a more substantial drop in balanced accuracy from 0.72 to 0.64, compared to Data Shapley’s more gradual decline, indicating better identification of crucial nodes across all classes. Similar patterns are observed on Citeseer, where PC-Winter’s balanced accuracy drops from 0.62 to 0.57, showing consistent performance across different class distributions. For Pubmed, PC-Winter achieves a significant drop from 0.74 to 0.65, further validating its effectiveness in identifying important nodes without class bias.

The steeper drops in balanced accuracy across all datasets demonstrate that PC-Winter effectively identifies nodes crucial for model performance while maintaining fairness across different classes. This analysis complements our main results by showing that PC-Winter’s superior performance

extends to class-balanced metrics, suggesting its robustness and applicability in scenarios where class balance is particularly important.

L INTEGRATION WITH P-SHAPLEY

Recent work by (Xia et al., 2024) proposed P-Shapley, which innovates on utility function design by utilizing probabilistic classifier outputs. We investigate how this utility-focused innovation interacts with our structural approach to graph data valuation by integrating P-Shapley’s probability-based utility function with both Data Shapley and PC-Winter frameworks.

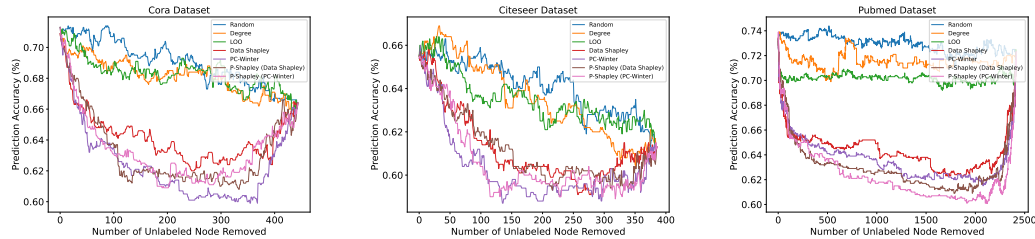


Figure 13: Performance comparison using different utility functions. The results show PC-Winter maintains its advantages regardless of utility function choice, while demonstrating complementary benefits from P-Shapley’s probability-based utility. From left to right: (a) Cora, (b) Citeseer, (c) Pubmed.

Our experimental results, shown in Figure 13, reveal several important insights about the relationship between structural innovations and utility function design in graph data valuation. Most notably, PC-Winter consistently outperforms Data Shapley regardless of utility function choice. On the Cora dataset, PC-Winter achieves minimum accuracies of 0.599 and 0.608 with standard and P-Shapley utilities respectively, compared to Data Shapley’s 0.620 and 0.625. This pattern holds across datasets, though with varying magnitudes.

The consistent performance advantage demonstrates that PC-Winter’s core innovation - its precedence-constrained formulation for handling graph dependencies - provides fundamental benefits independent of utility function design. The steeper performance drops in PC-Winter variants indicate more effective identification of crucial nodes, validating that our structural approach addresses fundamental challenges in graph data valuation.

Interestingly, P-Shapley’s probability-based utility function shows complementary benefits that vary by dataset. On Cora and Citeseer, integrating P-Shapley’s utility with PC-Winter leads to slightly improved node importance identification, while on Pubmed, the standard accuracy utility performs better. This dataset-dependent behavior suggests that while both structural and utility-based innovations offer benefits, they operate on different aspects of the data valuation problem.

These findings highlight the modularity of innovations in data valuation: improvements in handling graph structure (like PC-Winter) can be effectively combined with advances in utility function design (like P-Shapley). While both approaches contribute to better data valuation, our results suggest that addressing the structural challenges of graph data provides consistent benefits across different evaluation frameworks.

M PC-WINTER FRAMEWORK OVERVIEW

Figure 14 presents an overview of the PC-Winter framework for graph data valuation. The framework operates on an inductive setting, where the input graphs are divided into three mutually exclusive structures: the Training Graph, the Validation Graph, and the Testing Graph.

The Training Graph contains the elements to be evaluated and is the main focus of the PC-Winter algorithm. Within this graph, nodes labeled as l (l_0, l_1) represent labeled nodes, nodes labeled as w ($w_0 - w_3$) represent 1-distance neighbors of labeled nodes, and nodes labeled as u ($u_0 - u_6$) represent

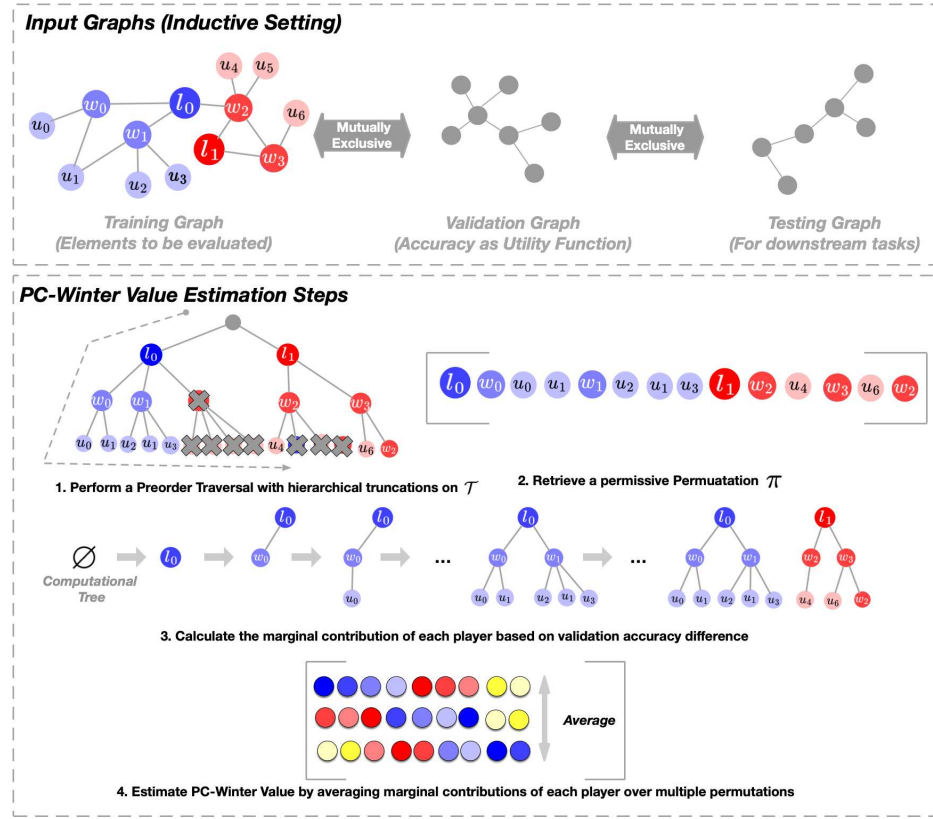


Figure 14: PC-Winter Framework Overview

2-distance neighbors of labeled nodes. This hierarchical structure aligns with the concept of the Computation Tree introduced in Definition 1 (Section 2.3).

The Validation Graph is used for calculating the accuracy of the GNN model, which serves as the utility function in the PC-Winter framework (Definition 3, Section 3.1). The Testing Graph is reserved for downstream tasks, such as the node dropping experiments conducted in Section 4.2.

PC-Winter Value Estimation Steps:

1. Perform a Preorder Traversal with hierarchical truncations on the Computational Tree \mathcal{T} . This step generates permissible permutations that respect the Level and Precedence Constraints (Section 3.3, Theorems 1 and 2). The hierarchical truncation strategy (Section 3.4.2) is applied to reduce computational complexity while maintaining valuation quality.
2. Retrieve a permissive Permutation π from the Preorder Traversal. Each permutation represents a unique ordering of the players (nodes) in the Training Graph.
3. Calculate the marginal contribution of each player based on the validation accuracy difference. This step involves retraining the GNN model on subgraphs induced by the permutation and measuring the change in accuracy when a player is added (Definition 3, Section 3.1). The local propagation strategy (Section 3.4.3) is employed to efficiently compute these marginal contributions.
4. Estimate the PC-Winter Value by averaging the marginal contributions of each player over multiple permutations. The permutation sampling strategy (Section 3.4.1) is used to approximate the PC-Winter value (Equation 3, Section 3.2) by considering a subset of permutations.

The PC-Winter framework provides a comprehensive approach to graph data valuation by incorporating graph-specific constraints and efficient approximation strategies. The framework's design allows for the accurate quantification of the importance of individual graph elements (nodes and

edges) while considering their complex interdependencies and contributions to the GNN model’s performance.

Table 9: Key Notations Used in the Paper

Notation	Definition	Description
$\mathcal{G} = \{\mathcal{V}, \mathcal{E}\}$	Graph	Original graph with node set \mathcal{V} and edge set \mathcal{E}
$\mathcal{V}_l \subset \mathcal{V}$	Labeled Node Set	Set of nodes with known labels
\mathcal{P}	Player Set	Union of nodes from computation trees of all labeled nodes (Definition 2)
T_i^K	K-level Computation Tree	Computation tree of depth K rooted at node v_i (Definition 1)
$\mathcal{D}(p)$	Descendants	Set of descendants of player p in the contribution tree
Ω	Permissible Permutations	Set of permutations satisfying both Level and Precedence constraints
P_i^π	Predecessor Set	Set of players appearing before player i in permutation π
$U(\cdot)$	Utility Function	Model performance on validation set (Definition 3)
$\psi_p(\mathcal{P}, U)$	PC-Winter Value	Value of player p based on permissible permutations
r_1, r_2	Truncation Ratios	Hierarchical truncation ratios for first and second-hop neighbors
v_i	Node	A node in the original graph \mathcal{G}
x_i	Node Features	Feature vector of node v_i
y_i	Node Label	Label of node v_i
C	Label Set	Set of possible labels for nodes
d	Feature Dimension	Dimensionality of node feature vectors
$h_i^{(k)}$	Node Representation	Learned representation of node v_i at the k -th GNN layer
W	Weight Matrix	Learnable weight matrix in GNN layers
$N(v_i)$	Neighbors	Set of neighboring nodes of node v_i
$deg(v_i)$	Node Degree	Number of edges connected to node v_i
$G_{in}(S)$	Node-Induced Graph	Graph induced by a subset of players $S \subset \mathcal{P}$
$A(\cdot)$	GNN Model	Graph Neural Network model trained on a given graph
$acc(\cdot)$	Accuracy Function	Function measuring the accuracy of a trained GNN model
\mathcal{T}	Contribution Tree	Tree structure representing hierarchical contributions of players
$\Pi(\mathcal{P})$	Permutations	Set of all possible permutations of player set \mathcal{P}
π	Permutation	A specific permutation of players
$\pi[i]$	Permutation Rank	Positional rank of player i in permutation π
Ω_s	Sampled Permutations	A subset of permissible permutations sampled for approximation

N NOTATION TABLE

To facilitate a better understanding of our methodology and theoretical framework, we present a comprehensive table of notations at Table 9 used throughout this paper. The notations cover various aspects of our work, including graph structures, neural network components, computational trees, and permutation-related concepts. This systematic organization of notations aims to help readers track and understand the mathematical formulations and algorithmic components more effectively.

Additionally, we provide detailed descriptions for each notation to ensure clarity and precision in our mathematical expressions.

The notations are organized into several conceptual categories. The first category includes basic graph structural elements ($\mathcal{G}, \mathcal{V}, \mathcal{E}$) and node attributes (x_i, y_i). The second category covers computation tree-related notations ($T_i^K, \mathcal{D}(p)$), which are essential for understanding our hierarchical valuation framework. The third category encompasses permutation-related notations (Ω, π, P_i^π), which are crucial for the PC-Winter value computation. Finally, we include model-specific notations ($h_i^{(k)}, W$) and evaluation metrics ($U(\cdot), acc(\cdot)$) that are used throughout our theoretical analysis and experimental validation.